UNIVERSITY OF CALIFORNIA
SANTA CRUZ

FREE HOMOTOPY CLASSES IN SOME N-BODY PROBLEMS

A dissertation submitted in partial satisfaction of the
requirements for the degree of

DOCTOR OF PHILOSOPHY

in

MATHEMATICS

by

Connor Fox Jackman

June 2018

The Dissertation of Connor Fox Jackman
is approved:

Professor Richard Montgomery, Chair

Professor Jie Qing

Professor Debra Lewis

Tyrus Miller
Vice Provost and Dean of Graduate Studies

Table of Contents

Abstract

Free Homotopy classes in some N-body problems

by

Connor Fox Jackman

In this thesis we study two types of planar N-body problems: the motion of N point masses in a plane under a strong force law of attraction and under Newton's law of attraction. We aim to understand these orbits by which free homotopy classes are realized in the configuration space.

The first part looks at the strong force law of attraction: where the force is proportional to the inverse cube of the mutual distances. This problem is especially suited to the Jacobi-Maupertuis principle, which reformulates the problem as a complete geodesic flow in $\mathbb{C}P^{N-2}$ with collisions deleted. Montgomery [54] found negatively curved circumstances for such a 3-body problem, and consequently the orbits could be described effectively by symbolic dynamics and free homotopy classes are realized uniquely. Here we show that the extension to $N > 3$ is not so straightforward: the sectional curvatures have mixed signs, positive in some places and negative in others however, when restricting attention to the collinear 4-body strong force problem we do find negatively curved circumstances allowing us to describe such orbits as geodesics in the hyperbolic plane.

The second part examines the force law of Newton: where the force is proportional to the inverse square of the mutual distances. This classic problem has been well studied. Féjoz [25, 26] has established the existence of periodic and quasiperiodic orbits in the lunar

regions using perturbation methods. Here we describe these orbits using 'syzygy sequences' to represent the homotopy classes realized in these lunar regions. Our method of proof is to show that orbits of the unperturbed problem that avoid certain isolated tangencies retain their homotopy class in the full perturbed problem.

Dedicated to Mom, Dad, Bella, Eddie and Tails.

Acknowledgments

I cannot thank enough Richard Montgomery, whose patience, careful hints and math walks in the Santa Cruz hills taught me a lot of mathematics and who by example taught me a lot about being a nice person. Also Jacques Féjoz, who patiently explained to me how one works with the coordinates of celestial mechanics and the KAM theory and whose hospitality and excellent cooking during my stay in France was greatly appreciated.

I am also grateful to the advice of Rick Moeckel, who encouraged me to pursue the consequences of the negative curvature in the collinear problem, as well as Holger Dullin, who saved me from lots of troubles by suggesting to 'project the tangencies' in determining the syzygy sequences of uncoupled Kepler problems. This work has also benefited greatly from the interest and help of Josué Meléndez in the curvature techniques and for providing comida corridas and a nice game of hoops during a productive visit to UAM. I also thank Wei Yuan for his helpful interest in my work and suggestions to explore the holomorphic curvature properties.

The support of my friends and office mates: Richard Gottesman, Joe Ferrara, Gabe Martins, Sisi Song, Victor Bermudez, Patrick Allmann and Robert Hingtgen, among others, has kept my motivation up whether it be through filling the kitchen at Calvin place with math talk or long day hikes to clear our minds. I am also grateful to the Chateaubriand fellowship, which allowed me the opportunity to visit the IMCCE group in Paris. The lively lunch conversations of Alain Albouy, Alain Chenciner, Guo Wei Yu and Thibaut Castan in particular inspired me to push myself to learn and appreciate more dynamics and astronomy.

The editing help of Kim Crisci and especially the sharp eyes of Alan Plummer was

greatly appreciated, as well as that of Diana Gonzalez Santillan, who patiently looked at each draft as if it was new and taught me how to scan pictures.

Chapter 1

Introduction

In the following we consider questions relating to 'shapes' of orbits in some *planar* N-body problems. When there are three bodies this shape is captured by the oriented triangle they form: changing orientation requires an instant of syzygy, an astronomical term for collinearity (see figure 1.1). Therefore to keep track of an orbit's shape one may list the syzygy types in temporal order.

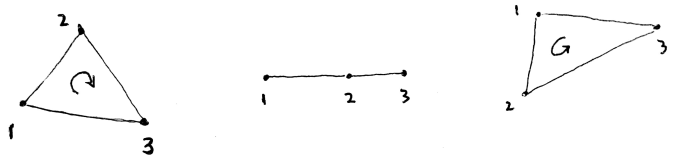

Figure 1.1 Changing orientation by passing through a '2' syzygy.

1.1 Some history

Before jumping into the mathematics, let us take a moment to appreciate the gravity of our situation. Celestial mechanics and the N-body problem have an interesting development and strong influence on science and mathematics (see for example [21, 16, 17, 23, 24]). In this section, we recall a few seminal points.

One encounters the interplay of observation and theory in the imaginative explanations of the motions of the wandering stars. These explanations were refined as observations became more precise −notably Galileo's observation of Jupiter's moons and Brahe's careful records of the motion of Mars, which culminate with Kepler's laws. Kepler's laws will be seen as consequences of Newton's inverse square attraction, which succeeded in giving a complete picture of a two body system and confirmed, for example, the prediction of Halley's comet. However, more than two body systems will continue to give 'headaches' until the development of perturbation theory, which will lead to a great confirmation of Newton's equations. Le Verrier and Adams predict the coordinates of a new planet by analyzing perturbations in the orbit of Uranus. Galle then observes the planet Neptune at these predicted coordinates! Peculiarities in the perihelion position of Mercury are analyzed as well, leading to the search for another inner planet, Vulcan, which is never found. Mercury's peculiarities will be understood as the scientific frontier extends to relativity theory.

Nevertheless, while a theory may lose its relevance for dealing with the general case, it need not lose its charm or usefulness. Indeed, Poincaré demonstrates that the classical three body problem exhibits complicated behavior, drawing the focus towards a qualitative under-

standing of the orbits. This has influenced the development of dynamical systems, analysis, and topology for instance. Moreover, the classic theory continues to hold interest not just for mathematics, but for space exploration and science fiction (e.g. [20, 46]) as well.

The evolution of an orbit's 'shape' is part of this qualitative study initiated by Poincaré [61]. Hadamard [33] found that the orbit of a free particle on a surface was strongly influenced by the curvature of the surface, in particular obtaining strong qualitative results for negatively curved surfaces and posing:

"Les circonstances que nous venons de recontrer se retrouveront-elles dans d'autres problèmes de Mécanique? Se prèsenteront-elles, en particulier, dans l'étude des mouvements des courps célestes? C'est ce qu'on ne saurait affirmer. Il est probable, cependant, que les résulatats obtenus dans ces cas difficiles seront analogues aux précédents, au moins par leur complexité."[1]

Montgomery in [54] found such negatively curved circumstances for a certain strong force 3-body problem. In this work we first examine the curvature for a strong force 4-body problem, finding some negatively curved circumstances. Next we consider a Newtonian force and study the shapes arising from orbits in the classical lunar regions as described by Féjoz in [26].

In the remaining sections of this introduction, we will state our results regarding these two approaches. But first we define the shape sphere.

[1] May the circumstances which we have encountered be found in other mechanical problems? Do they appear for example in celestial mechanics? It is difficult to be certain. However, it is likely that the results obtained in these difficult cases are similar to the preceding ones, at least as regards their complexity.

1.2 Shape sphere

Details on the shape sphere can be found in [55, 52]. The goal is to track the positions of $N \in \mathbb{N}$ weighted points in a plane as they move according to a law of motion.

First identify the plane with the complex numbers $\mathbb{C}$ and write the position of the body of mass m_j as $q_j \in \mathbb{C}$ for $j = 1, ..., N$. In what follows, the law of motion consists of taking some homogeneous of degree $-\alpha$ *potential function*[1] such as $U_\alpha = \sum_{i<j} \frac{m_i m_j}{|q_i - q_j|^\alpha}$, then the equations of motion can be written as

$$\ddot{q} = \nabla U_\alpha, \tag{1.1}$$

where $q = (q_1, ..., q_N) \in \mathbb{C}^N \backslash \{q : U(q) = \infty\}$ and ∇ is the gradient with respect to the *mass metric* on $\mathbb{C}^N$:

$$\langle v_1, ..., v_N; w_1, ..., w_N \rangle_{mm} := \Re(\sum_{j=1}^{N} m_j v_j \overline{w}_j).$$

Curves in this configuration space can be represented by braids (see figure 1.2).

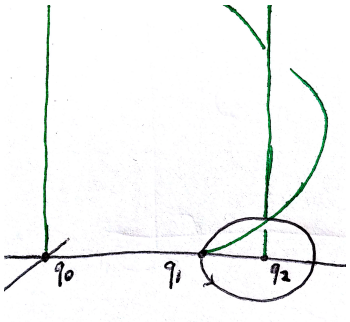

Figure 1.2 One may lift the curve $\gamma(t) = (\gamma_1(t), ..., \gamma_N(t))$ to the braid with strands $(\gamma_i(t), t) \in \mathbb{C} \times [0, 1]$. Note that deleting the collisions ensures that the braid remains free from self-intersections.

[1] For $\alpha = 0$ it is more interesting to take $U_0 = \sum_{i<j} m_i m_j \log |q_i - q_j|$.

However, as space has no preferred coordinate system, it is more natural to consider the reduced configuration space, up to choice of origin

$$q \mapsto q + (\lambda, ..., \lambda), \quad \lambda \in \mathbb{C},$$

and once an origin is chosen up to choice of axes from this origin

$$q \mapsto (e^{i\theta} q_1, ..., e^{i\theta} q_N), \quad \theta \in S^1.$$

Via the mass metric, we will identify $\mathbb{C}^N/\mathbb{C}$ with the center of mass zero space: $(1, ..., 1)^{\perp} \cong \mathbb{C}^{N-1}$, and then $\mathbb{C}^{N-1}/S^1$ with $\mathbb{C}P^{N-2} \times \mathbb{R}_{\geq 0}$ by $z \mapsto (\mathbb{C}^* z, \|z\|_{mm})$, where $\mathbb{C}^* z$ is the complex line spanned by z. Recall that having deleted the *collisions* $\Delta := \{q : U(q) = \infty\}$ from $\mathbb{C}^N$, the corresponding points are deleted from these quotients as well. We call

$$\mathbb{C}P^{N-2} \backslash P\Delta$$

the *shape sphere* and keep track of an orbits shape by projecting it down to a curve on the shape sphere. What sorts of curves arise from projecting down solutions of eq. (1.1)?

EXAMPLE: When $N = 3$ the shape sphere is $\mathbb{C}P^1$ minus three points (for the $\binom{3}{2}$ binary collisions). We may see the reductions in coordinates as follows. Projecting orthogonally onto the center of mass zero space in *Jacobi coordinates*:

$$(q_0, q_1, q_2) \overset{Jacobi}{\mapsto} \left(\frac{q_0 - q_1}{\sqrt{1/m_0 + 1/m_1}}, \frac{q_2 - \frac{m_0 q_0 + m_1 q_1}{m_0 + m_1}}{\sqrt{1/(m_0 + m_1) + 1/m_3}}\right) = (z_1, z_2) \in \mathbb{C}^2,$$

takes care of translations. For rotations and dilations, the coordinates on $\mathbb{C}P^1$ arising from the Hopf map: $(z_1, z_2) \overset{affine}{\mapsto} z_1/z_2 = w \overset{stereo}{\mapsto} \left(\frac{|w|^2 - 1}{1 + |w^2|}, \frac{2w}{1 + |w|^2}\right)$, or

$$(z_1, z_2) \overset{Hopf}{\mapsto} \left(\frac{|z_1|^2 - |z_2|^2}{|z_1|^2 + |z_2|^2}, \frac{2 z_1 \bar{z}_2}{|z_1|^2 + |z_2|^2}\right) \in S^2$$

will coordinatize our shape sphere. In these coordinates, the equator of the sphere represents collinear configurations (see figure 1.3). A curve on this shape sphere is coded by its *syzygy sequence*: we list in temporal order the crossings with the collinear equator, giving each arc of the equator the symbol representing the body in the middle.

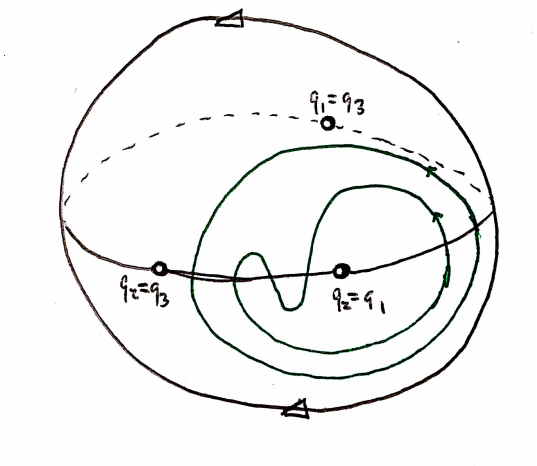

Figure 1.3 The shape sphere when $N = 3$. Here the poles represent oriented equilateral triangles and the equator corresponds to the collinear shapes. We have drawn two homotopic curves having syzygy types $\overline{12}$ and $\overline{1222}$.

We will mainly be interested in the closed curves that arise as solutions of eq. 1.1 up to homotopy. For syzygies this amounts to canceling consecutive symbols or *stutters*, e.g. $1222 \sim 12$. With $N = 3$ and a strong force it was found in [54] that almost every class (more specifically the tied classes, see figure 1.4 below) is realized *uniquely* by a stutter free solution. As for the $N = 3$ Newtonian force case it was found in [53] that (provided the angular momentum is non-zero) *every* class is realized by some solution.

1.3 Overview of strong force results

In §2 we will study the *strong force* problem (taking $\alpha = 2$ in eq. 1.1). This represents an inverse cube force which possesses some convenient features other than not being as heavily studied as the Newtonian force. First, any force field which is homogeneous of degree -3 can be reduced by a scaling (see [1]), which allows us to reduce the dimension by one as well as to focus on the *zero energy level* to find periodic orbits. Second, as noticed by Poincaré [60] (see also [29, 30]) the action goes to infinity as one approaches a collision.

Indeed let r be the mutual distance going to zero and note that the dominant term of $\ddot{r}$ is like $-1/r^3$ so that $\ddot{r}\dot{r} \sim -\dot{r}/r^3$ and integrating gives $(\dot{r})^2 \sim 1/r^2$ or $rdr \sim dt$. The action $\int (h+2U)\, dt$ is dominated by the term $1/r^2$ of U and so behaves like:

$$\int r^{-2} dt \sim \int r^{-1} dr \sim \log(r),$$

which goes to infinity as $r \to 0$. Consequently, minimizing over a tied homotopy class (see figure 1.4) yields at least one solution in this homotopy class.

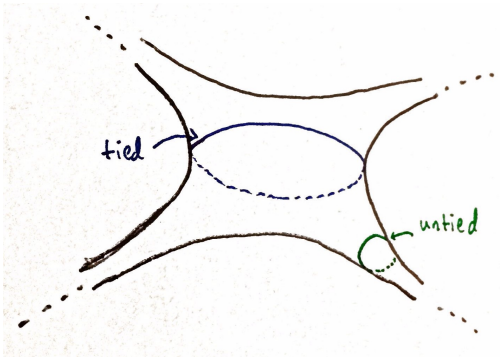

Figure 1.4 A tied homotopy class versus an untied class on a surface. Informally, a class is tied if it cannot be moved to infinity without its length becoming infinite (see [29] def 1.2).

Similarly, in spherical coordinates near a collision the Jacobi-Maupertuis (or JM-metric see §2 below) metric has length as $r \to 0$ asymptotic to

$$\int \sqrt{(h + r^{-2})(dr^2 + O(r^2))} \sim \int r^{-1}\, dr,$$

which goes to infinity as we approach collision and so is complete in this case (see [54]).

In [54], the curvature of this strong force JM-metric on the shape sphere with three equal masses was shown to be negative almost everywhere. Geodesic flows on negatively curved surfaces have long been studied [33, 35, 8] as examples of symbolic dynamics and sensitive dependence on initial conditions (see also appendix B). In particular a consequence of Montgomery's computation is that the minimizing periodic orbits which realize the tied classes are unique, i.e. the (stutter free) syzygy sequence of a periodic orbit is unique to it.

The goal is then to extend Montgomery's results by relating the differential geometry of this JM-metric to dynamical properties of the strong force zero energy problem for $N > 3$. We first find:

Theorem 1. *([39]) The sectional curvatures of the JM-metric on the shape sphere have mixed signs for $N > 3$.*

Which is somewhat disappointing, as manifolds of mixed curvature are not as widely studied as those of fixed sign. The positive curvature is found in the orthogonal directions to the collinear configurations. However, this mixed curvature does not preclude the possibility that realizing orbits of a homotopy class may be unique, which remains an open question.

We next find some dynamical consequences of our curvature computations by focusing on some totally geodesic surfaces of the equal masses $N = 4$ case. These surfaces arise as

the fixed point sets of isometries.

Theorem 2. *([38]) The JM-metric restricted to the reduced collinear 4-body strong force problem has strictly negative curvature. Consequently, there exists a unique collinear solution connecting any two realizable binary (or double binary) collisions.*

Also in [38] Josué Meléndez computed the curvature for the parallelogram 4-body problem, showing it is a 'shirt' (see figure 1.4) of negative curvature.

Last we return upstairs to the configuration space, $\mathbb{C}^N \backslash \{\text{collisions}\}$ and in a more general setting find a relation between the curvature over certain complex planes and central configurations:

Theorem 3. *([37]) Consider any $\alpha \neq 0$ and masses $m_i > 0$ and endow $\mathbb{C}^N \backslash \Delta$ with the JM-metric at energy level $H = h$. Then q_0 is a central configuration if and only if the holomorphic sectional curvature and Kobayashi sectional curvatures agree on the plane $\mathbb{C}q_0$. These curvatures then have the value*

$$-\frac{h\alpha^2 U(q_0)}{2(h+U(q_0))^3 \|q_0\|^2}.$$

REMARKS: One can use these computations to extend the instability results of [7] to conclude the instability of certain homographic motions: namely those with negative sectional curvatures over their motion, or in other words the sectional curvatures are negative through some family of planes $\sigma(t) \ni \dot{q}(t)$.

When $h = 0$, the holomorphic sectional curvature is non-positive and vanishes exactly along the fibers (complex span) of central configurations. When $\alpha = 2$ and $h = 0$ we may

quotient out these fibers of zero curvature to get a metric on the shape sphere: does the non-positive holomorphic sectional curvature persist on the shape space for $h = 0, \alpha = 2$ and would there be any dynamical consequences of this?

1.4 Overview of Newtonian force results

In §3, we will examine some syzygy sequences arising in the classical 3-body problem (that is with $\alpha = 1$ in eq. (1.1)). In the Newtonian case the existence of orbits realizing given free homotopy classes was solved positively by Montgomery and Moeckel [53] using blowup techniques (see [49]). For small non-zero angular momentum and equal or nearly equal masses, they show that every class is realized.

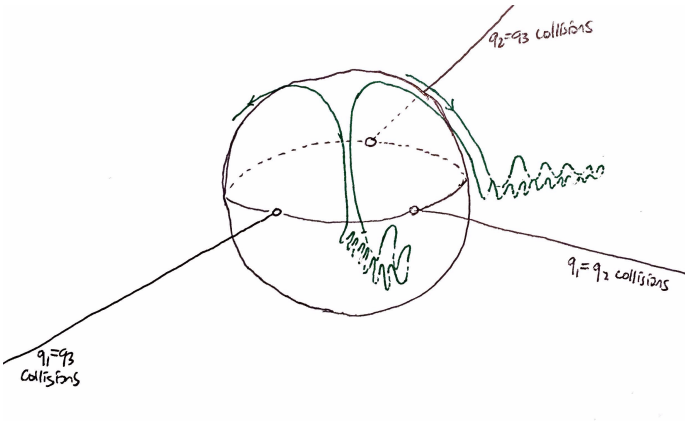

Figure 1.5 The realizing solutions of [53] in the space $S^2 \times \mathbb{R}_{\geq 0}$ where we draw the triple collision sphere $S^2 \times \{0\}$ enlarged. By wobbling around an Euler central configuration, these solutions pick up many stutters of a certain type. They transfer to another Euler configuration to wobble around by passing close to triple collision near a Lagrange central configuration.

On the other hand, there are many known periodic or quasi-periodic solutions arising

out of perturbation methods. Such solutions will differ from those of [53], in that they will be far from triple collision. Can we find which syzygy sequences are realized from these perturbation methods? We are also motivated by Montgomery's existence question:

Does there exist a solution to the Newtonian three body problem with zero angular momentum and equal masses realizing the syzygy sequence $(01)^K$ *for some* $K \in \mathbb{N}$*?*

If one considers two uncoupled Kepler problems with equal masses, then the angular momentum will be zero only when the two orbits intersect, continuing such orbits to the full three-body problem would involve analyzing the 'second species solutions' (see [47]). Here, as a first step, we examine some syzygy sequences arising from the orbits described by Féjoz [25, 26] in the 'perturbing region'. This region's configurations consist of certain *nested* ellipses where the outer body is far away (the lunar region) or an outer and inner mass are small (the planetary region). As the ellipses are nested, the orbits remaining in the perturbing region can only reduce to a sequence $\overline{01}$ or the empty sequence.

Theorem 4. *For angular momentum zero there exist periodic orbits realizing the sequence* $(01)^K$ *without stutters. These solutions have an outer body with small mass and an inner orbit that is nearly a circular Keplerian orbit.*

In the lunar regions there are near inner collision orbits where the inner body switches from prograde to retrograde motion by passing through a degenerate collision ellipse. Such orbits have angular momentum non-zero and syzygy sequences of the form

$$...(10)^{a_0}(01)^{a_1}(10)^{a_2}...$$

with $a_i \in \mathbb{N}$ *and* $a_i = O(a^{-3})$ *where* $a << 1$.

REMARKS: The near inner collision orbits can be seen as an extended description of the orbits found in [41], where the near innner collision syzygy sequences of theorem 4 are established on a finite time scale whereas in theorem 4 we show that in certain cases such sequences can be continued for all time.

In the lunar regions there are also quasi-periodic or periodic orbits realizing the sequence $(01)^K$, some of which may have equal masses and *non-zero* angular momentum. The syzygy sequences of these orbits have the same forms as in theorem 4. In general one may continue a syzygy sequence of the Keplerian or secular dynamics from these lunar regions, *provided* one avoids certain isolated 'tangencies' that cause extra stutters in the sequences of theorem 4. Is it possible any of these continued solutions could reduce to the empty sequence, or in other words: can we find an orbit which unwinds itself?

Chapter 2

Strong Force

Here we present the proofs of results outlined in §1.3, taking the 'metric approach'. Our motivation [54] takes this metric approach in the case $N = 3$ and we are concerned primarily with examining this approach in the $N = 4$ case. The first order of business is to define the metric of interest.

2.1 The metric on the reduced space

The Jacobi-Maupertuis (or JM) principle is a least action principle for Hamiltonian flows restricted to a regular level set of the energy.

JM-principle: *Let (M, ω) be a symplectic manifold and consider the Hamiltonian flow of $H \in C^\infty(M)$. Then on a regular level set of H, and for a (local) primitive λ of ω, the Hamiltonian flow lines are extremals of the action $\gamma \mapsto \int_\gamma \lambda$ among fixed endpoint variations*

staying in this level set.

Proof: In local coordinates, the flow on a regular level set $H = h$ is the Reeb flow of λ. Take local Darboux coordinates $(x_1, y_1, ..., x_{n-1}, y_{n-1}, z)$, with $\lambda = \sum x_i dy_i + hdz$ and the Hamiltonian vector field given by $\frac{\partial}{\partial z}$ (see [4]).

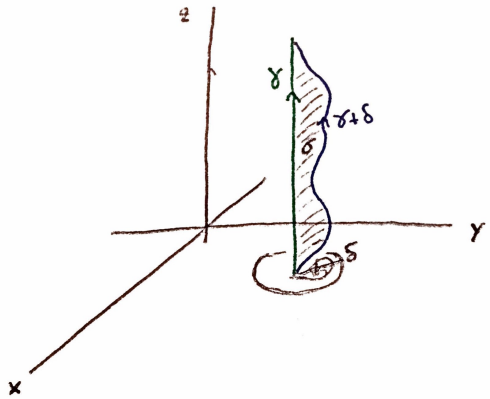

Figure 2.1

Let $\gamma(t) = (x, y, z(t))$ be a solution curve in these coordinates and $\gamma+\delta$ a fixed endpoint variation of γ (see figure 2.1). Take a surface σ with $\partial\sigma = \{\gamma\} \cup \{\gamma+\delta\}$, so that by Stokes' theorem

$$\int_{\gamma+\delta} \lambda - \int_{\gamma} \lambda = \int_{\sigma} \omega = \text{sum of areas of projections onto } (x,y) \text{ planes } = O(\delta^2).$$

□

When we have a natural system, the Legendre transform renders the Lagrangian or Hamiltonian frameworks equivalent, and the JM-principle can be restated as follows (see [4] pg. 247):

Metric form: *Consider a manifold Q with Riemannian metric g and potential function $U \in C^\infty(Q)$. The extremals associated to the Lagrangian $L = \frac{1}{2}g + U$ having fixed energy $h = H = \frac{1}{2}g^\# - U$ are up to reparametrization geodesics of the metric $(h+U)g$ on Q.*

Applying these considerations to the strong force with our mind towards periodic solutions, we find the zero energy level of interest. Due to the potential's homogeneity of degree -2, the virial identity reads as

$$\ddot{I} = 4H,$$

where $I = \|q\|^2_{mm}$ is the *moment of inertia*. In particular, periodic orbits are only possible when $H = 0$. With equal masses, this zero energy metric of interest is then the conformally flat

$$d\bar{s}^2 = U ds^2_{Eucl} \tag{2.1}$$

on $\mathbb{C}^N \backslash \Delta$.

We will also study the curvature of this metric after reductions by translations and complex scaling:

$$\mathbb{C}^N \backslash \Delta \to \mathbb{C}^{N-1} \backslash \Delta \to \mathbb{C}P^{N-2} \backslash P\Delta,$$

where the first submersion is due to the metric's invariance under translations and the second due to the invariance under complex scaling. Note that the homogeneity of degree -2 for the strong force allows the additional dilation symmetry.

As each reduction is a symmetry of the metric $d\bar{s}^2$, we may define a metric, ds^2_{JM}, on the shape sphere via Riemannian submersion. Such geodesics then correspond to the push

down of horizontal geodesics upstairs i.e. perpendicular to the fibers. The translation fiber is $\text{span}_{\mathbb{C}}\{(1,...,1)\}$, so that we may simply consider solutions in center of mass zero coordinates. The second quotient has fiber $V_q = \text{span}_{\mathbb{C}}\{q\}$, so that horizontal geodesics satisfy the additional conditions

$$\dot{I} = \langle q, \dot{q} \rangle = 0,\ C = \langle iq, \dot{q} \rangle = 0,$$

where C is the angular momentum.

Upstairs on $\mathbb{C}^N$ or $\mathbb{C}^{N-1}$ we will denote the sectional curvature of $d\bar{s}^2$ at q through the plane σ by $K_q(\sigma)$. Downstairs on $\mathbb{C}P^{N-2}$, we must add in the bracket term from O'Neill's submersion formula (see appendix B eq. 3.9) and denote the downstairs sectional curvature of ds^2_{JM} by $\mathcal{K}_{[q]}([\sigma])$.

2.2 Curvature computations

We first consider sectional curvatures on the reduced space, $\mathbb{C}P^{N-2}\backslash P\Delta$. The computations may be manageably done over some invariant surfaces, for instance when $N = 4$ over the collinear configurations, which are the fixed set of the isometry $q \mapsto \overline{q}$ and project down to an $\mathbb{R}P^2\backslash P\Delta$.

Proposition 2.2. *For $N = 4$, we have $\mathcal{K}_{\mathbb{R}P^2}(T\mathbb{R}P^2) < 0$ and at the collinear central configurations that $\mathcal{K}_{\mathbb{R}P^2}(iT\mathbb{R}P^2) > 0$.*

Proof: We will first show that $\mathcal{K}_{\mathbb{R}P^2}(T\mathbb{R}P^2) < 0$. Take the coordinates:

$$2\xi_1 = q_1 - q_2 - q_3 + q_4,\ \ 2\xi_2 = q_1 - q_2 + q_3 - q_4,\ \ 2\xi_3 = q_1 + q_2 - q_3 - q_4, \tag{2.3}$$

where we have

$$U = \sum_{1 \le i < j \le 3} \frac{1}{|\xi_i - \xi_j|^2} + \frac{1}{|\xi_i + \xi_j|^2},$$

for $\xi_j = x_j + iy_j \in \mathbb{C}$ and $j = 1,2,3$.

Reducing the collinear configurations by dilations and rotations amounts to restricting the metric

$$U|_{\mathbb{R}^3}(dx_1^2 + dx_2^2 + dx_3^2)$$

to the sphere $I = 1$ (with antipodal points identified).

That is, in the usual spherical coordinates ($I = \rho^2$), we wish to compute the curvature, K_C, of

$$\hat{U}I(d\phi^2 + \cos^2\phi d\theta^2),$$

where $\hat{U} := U|_{\mathbb{R}^3}$. Set $u = \hat{U}I = U|_{S^2}$.

Using isothermal coordinates and that the general formula for the curvature of $\phi(dx^2 + dy^2)$ is $-\frac{\Delta \log \phi}{2\phi}$, we have:

$$uK_C = 1 - \frac{1}{2}\Delta_{S^2} \log u,$$

where Δ_{S^2} is the Laplacian on the sphere.

As:

$$\Delta_{S^2} \log u = (\Delta \log \rho^2 \hat{U})|_{S^2} = (\Delta \log \hat{U})|_{S^2} + 2,$$

where Δ is the standard Laplacian on $\mathbb{R}^3$, we see $K_C < 0$ is equivalent to $(\Delta \log \hat{U})|_{S^2} > 0$.

Hence it suffices to show that $\Delta \log \hat{U} > 0$.

It is easy to check that when $V \subset \mathbb{C}^M$ is an affine subvariety and $f : \mathbb{C}^M \backslash V \to \mathbb{C}^{M'} \backslash 0$ is holomorphic, that $\sum_{j=1}^{M} \frac{\partial^2 \log \|f\|^2}{\partial z_j \partial \bar{z}_j} \ge 0$. Moreover, the inequality is strict when $M' > 1$ and

$\frac{\partial f}{\partial z_j} \neq \lambda f$ for any $\lambda \in \mathbb{C}$ and some $j \in \{1,..,M\}$ (see eq. 2.7 below).

Hence setting $f_{ij}^{-}(\xi_1,\xi_2,\xi_3) = 1/(\xi_i - \xi_j), f_{ij}^{+}(\xi_1,\xi_2,\xi_3) = 1/(\xi_1 + \xi_j)$ and $\phi = \log U = \log \|f\|^2$ we have

$$\Delta_{\mathbb{C}^3}\phi := \sum_{j=1}^{3} \frac{\partial^2\phi}{\partial x_j^2} + \frac{\partial^2\phi}{\partial y_j^2} > 0.$$

Take $x = (x_1,x_2,x_3)$ and $y = (y_1,y_2,y_3)$. The symmetry $\phi(x,y) = \phi(y,x)$ implies

$$\frac{\partial^k\phi}{\partial x_j^k}(x,y) = \frac{\partial^k\phi}{\partial y_j^k}(y,x).$$

Now since $\phi(x,0) = \phi(0,x) = \phi(x,x) + const.$, we have

$$2(\frac{\partial^2\phi}{\partial x_j^2}(x,x) + \frac{\partial^2\phi}{\partial y_j^2}(x,x)) = \frac{\partial^2\phi}{\partial x_j^2}(x,0),$$

and so

$$\Delta \log \hat{U} = 2\Delta_{\mathbb{C}^3}\phi(x,x) > 0$$

as desired.

It remains to demonstrate some positive curvature. Let $v_a = v_a^i \partial_{x_i}$ be orthonormal and tangent to the $I = 1$ sphere contained in $\mathbb{R}^3 = (x,0)$. We will use the equation (see appendix B eq. 3.8)

$$U^3 \mathcal{K}(\sigma) = -\frac{U}{2}(\partial_1^2 U + \partial_2^2 U) + \frac{3}{4}((\partial_1 U)^2 + (\partial_2 U)^2) - \|\nabla U/2\|^2,$$

where $\sigma \subset \mathbb{C}q^{\perp}$ is spanned by the ds^2 orthonormal vectors $u_a = iv_a$, and $\partial_a f = df(u_a)$. Note that O'Neill's bracket term (eq. 3.10 in appendix B) is zero because of the $u_1 \cdot iu_2$ factor vanishing at these real planes.

Observe that $\nabla U|_{(x,0)}$ is totally real, i.e. it is in the span of v_1, v_2 and $q = (x,0)$. Hence

$$U^3 \mathcal{K}(iT\mathbb{R}P^2) = -\frac{U}{2}\Delta_y U - \frac{1}{4}\|\nabla U\|^2$$

and

$$U^3\mathcal{K}(T\mathbb{R}P^2) = -\frac{U}{2}\Delta_x U + \frac{1}{2}\|\nabla U\|^2 - \frac{3}{4}(\nabla U \cdot q)^2.$$

Adding these last two expressions we have

$$U^3(\mathcal{K}(iT\mathbb{R}P^2) + \mathcal{K}(T\mathbb{R}P^2)) = -\frac{U}{2}\Delta U + \frac{1}{4}\|\nabla U\|^2 - 3U^2. \tag{2.4}$$

We conjecture that eq. 2.4 is non-negative over all of $\mathbb{R}P^2$ but will only show it here at the central configurations, where $\nabla U = -2U(q)q$ (recall $\|q\| = 1$).

At such points eq. 2.4 becomes

$$-\frac{U}{2}\Delta U - 2U^2$$

and one computes that $\Delta U = (4-2n)U$ so that eq. 2.4 is

$$(n-4)U^2,$$

which is zero here since $n = 4$. Hence at the collinear central configurations we have:

$$\mathcal{K}_{\mathbb{R}P^2}(iT\mathbb{R}P^2) = -\mathcal{K}_{\mathbb{R}P^2}(T\mathbb{R}P^2) > 0,$$

since we showed previously that $\mathcal{K}_{\mathbb{R}P^2}(T\mathbb{R}P^2) < 0$.

□

Proof of theorem 1: Proposition 2.2 proves theorem 1 for $N = 4$. For $N > 4$, and configurations near a quadruple collision the metric is dominated by the JM-metric terms corresponding to $N = 4$. Hence the signs of the sectional curvatures in these directions will retain the mixed signs found in proposition 2.2. For $N = 3$ and *non-equal* masses, it was shown in [54]

that the curvatures are mixed. Hence for $N > 3$ and non-equal masses we retain these mixed signs near triple collisions. $\square$

REMARK: In [38] Josué Melendez has also shown the curvature to be negative over the invariant parallelogram surfaces (see [15]: these are the fixed point set of $(q_1, q_2, q_3, q_4) \mapsto (-q_2, -q_1, -q_4, -q_3)$ and project down to a sphere minus 4 points). Recently, Melendez has computed that the invariant trapezoid surface (the fixed point set of $(q_1, q_2, q_3, q_4) \mapsto (\overline{q}_2, \overline{q}_1, \overline{q}_4, \overline{q}_3)$) has negative curvature as well.

Now we consider sectional curvatures upstairs through complex planes. By using a 'Schwartz-type principle' from [44] the computations over these complex planes become much more manageable. In what follows we may just as easily treat the general case and even obtain some explicit formulas for the sectional curvatures. Consider then any masses $m_i > 0$ with a general $1/r^\alpha$ potential and fix the energy at some level $H = h$.

For a complex plane σ define

$$H_q(\sigma) := \sup_{f \in \mathcal{H}(D, \mathbb{C}^N \setminus \Delta) \text{ with } f(0)=q, \mathbb{C}f'(0)=\sigma} \{\text{Gaussian curvature at } z = 0 \text{ of } f^* ds^2_{JM}\}, \qquad (2.5)$$

where $D \subset \mathbb{C}$ is a disk. We call $H_q(\sigma)$ *Kobayashi's sectional curvature* at q through σ (see [44]). The main tool for the proof of theorem 3 is the following:

Lemma 2.6. *Let $q \in \mathbb{C}^N \setminus \Delta$ and $v \in \mathbb{C}^N$. Complete v to an orthonormal complex mass metric basis $v_1 = v/\|v\|, v_2, ..., v_N$. Then*

$$K_q(\mathbb{C}v) = H_q(\mathbb{C}v) - \frac{\sum_{j=2}^N |\partial_j U|^2}{(h+U)^3}.$$

Proof: See appendix B. □

A central configuration (see [50]) is a configuration q_0 for which $z(t)q_0$ is a solution for some $z(t) \in \mathbb{C}$, i.e. the solution keeps the same shape, q_0, for all time evolving only by dilations and rotations. Substitution into the equations of motion yields the conditions $\nabla U(q_0) = \lambda q_0$ for some constant λ and $z(t)$ satisfies a $1/r^\alpha$ central force problem. Note that the rotation invariance of U implies the constant λ above is real.

For a central configuration q_0, the space $\mathbb{C}q_0$ is invariant and carries dynamics of a $1/r^\alpha$ central force problem. This problem has the JM-metric $(h + r^{-\alpha})dzd\bar{z}$, which has curvature $-\frac{\alpha^2 h r^{2\alpha-2}}{2(hr^\alpha+1)^3}$, making one direction of theorem 3 not too strange. It was a pleasant surprise to find that conversely a certain curvature value can in fact determine a central configuration!

Proof of theorem 3: As in Lemma 2.6, take an orthonormal basis with $v_1 = q/\|q\|$. Now we have:

$$H_q(\mathbb{C}q) = K_q(\mathbb{C}q) \iff 0 = \partial_j U(q) = \langle \nabla U(q), v_j \rangle, \text{ for } j > 1 \iff \nabla U(q) = \lambda q.$$

It remains then to find the explicit value for the curvature at such configurations. We will make use of the following general formula in the proof: let $g = (g_1, ..., g_k) : D \to \mathbb{C}^k$ be holomorphic, then

$$-\partial\bar{\partial}\log(c + \|g\|^2) = \frac{|\langle g, g' \rangle|^2 - \|g\|^2\|g'\|^2 - c\|g'\|^2}{(c + \|g\|^2)^2}. \tag{2.7}$$

Let $f : D \to \mathbb{C}^N$ be a holomorphic map with $f(0) = q$ and $f'(0) = \lambda v$ (later we will set $v = q$). Then Kobayahi's holomorphic sectional curvature (eq. 2.5) is the supremum over all such maps

of the Gaussian curvature of $f^*(h+U)ds^2 = (h+U(f(z))\|f'(z)\|^2 dzd\bar{z} =: 2\rho_f dzd\bar{z}$ at $z=0$. This Gaussian curvature is given by $-\frac{\partial\bar{\partial}\log\rho_f}{\rho_f}|_{z=0}$.

First we can see that the supremum is attained by a linear map $z \mapsto q+zv$ by considering

$$-\frac{\partial\bar{\partial}\log\rho_f}{\rho_f} = -\frac{\partial\bar{\partial}\log(h+U(f(z))}{\rho_f} - \frac{\partial\bar{\partial}\log\|f'(z)\|^2}{\rho_f}. \tag{2.8}$$

Using that $f=(f_1,...,f_N)$ is holomorphic (so $\bar{\partial}f_k=0$), the first term of (2.8) is

$$\rho_f^{-1}\left(\frac{(\sum\bar{\partial}_j U\overline{\partial f_j})(\sum\partial_k U\partial f_k)}{(h+U)^2} - \frac{\sum\partial_k\bar{\partial}_j U\partial f_k\overline{\partial f_j}}{h+U}\right),$$

which contains no second derivatives of f. As we have fixed $f(0)$ and $f'(0)$ up to complex scaling, when evaluated at $z=0$ this first term is then independent of choice of f.

By applying eq. 2.7 to the second term of (2.8), we obtain

$$\frac{|\langle f', f''\rangle|^2 - \|f'\|^2\|f''\|^2}{\|f'\|^4},$$

which by Cauchy-Schwartz achieves its supremum of 0 exactly when $f''(0)=\lambda f'(0)$, for instance when $f(z)=q+zv$.

To evaluate $H_q(\mathbb{C}v) = -2\frac{\partial\bar{\partial}\log(h+U(q+zv))}{(h+U(q))\|v\|^2}|_{z=0}$, set

$$g_{ij}(z) = \frac{\sqrt{m_i m_j}}{(q_i-q_j+z(v_i-v_j))^{\alpha/2}},$$

so that $U(q+zv)=\|g\|^2$ and

$$g'_{ij}(z) = -\frac{\alpha}{2}\frac{\sqrt{m_i m_j}(v_i-v_j)}{(q_i-q_j+z(v_i-v_j))^{1+\alpha/2}}.$$

Now taking $v=q$ we have $g'(0) = -\frac{\alpha}{2}g_{ij}(0)$, and so by eq. 2.7

$$-\partial\bar{\partial}\log(h+U(q+zq))|_{z=0} = -\frac{h\alpha^2 U(q)}{4(h+U(q))^2}.$$

Hence when q is a central configuration:

$$K_q(\mathbb{C}q) = H_q(\mathbb{C}q) = -\frac{h\alpha^2 U(q)}{2(h+U(q))^3\|q\|^2}.$$

□

2.3 The Collinear 4-body problem

Now we will enjoy a few fruits of our labor by finding some dynamical consequences of our curvature computations in the collinear 4-body problem. Roughly, since the collinear 4-body problem is a surface split up into invariant disks (each disk corresponding to an ordering of the masses) and each disk is negatively curved, we can show that the geodesics on each disk behave as in the hyperbolic plane.

Proof of theorem 2: Continue with the coordinates $\xi_j = x_j + iy_j$ of eq. 2.3. After the spherical projection:

$$u = \frac{x_1+x_2}{1-x_3}, v = \frac{x_1-x_2}{1-x_3}$$

of the $I = 1$ sphere, our metric $U(\sum dx_i^2)|_{S^2}$ becomes $\frac{\lambda}{2}(du^2+dv^2)$ with:

$$\lambda = \frac{1}{u^2} + \frac{1}{v^2} + \frac{16}{((u-1)^2+(v-1)^2-4)^2}$$
$$+\frac{16}{((u+1)^2+(v+1)^2-4)^2} + \frac{16}{((u+1)^2+(v-1)^2-4)^2}$$
$$+\frac{16}{((u-1)^2+(v+1)^2-4)^2}.$$

The $\mathbb{R}P^2$ of collinear shapes is divided into $12 = 4!/2$ open domains by the collision locus. All of these domains are isometric and resemble triangles, the interiors of which are specified by an ordering of the masses on the line (mod an overall flip due to a rotation by π) (see figure 2.2). We focus on one such domain T corresponding to the ordering $q_1 \leq q_2 \leq q_3 \leq q_4$. Here the boundary in u, v coordinates translates to:

$$u = 0 \iff q_1 = q_2,$$

$$v = 0 \iff q_3 = q_4,$$

$$w = (u-1)^2 + (v+1)^2 - 4 = 0 \iff q_2 = q_3.$$

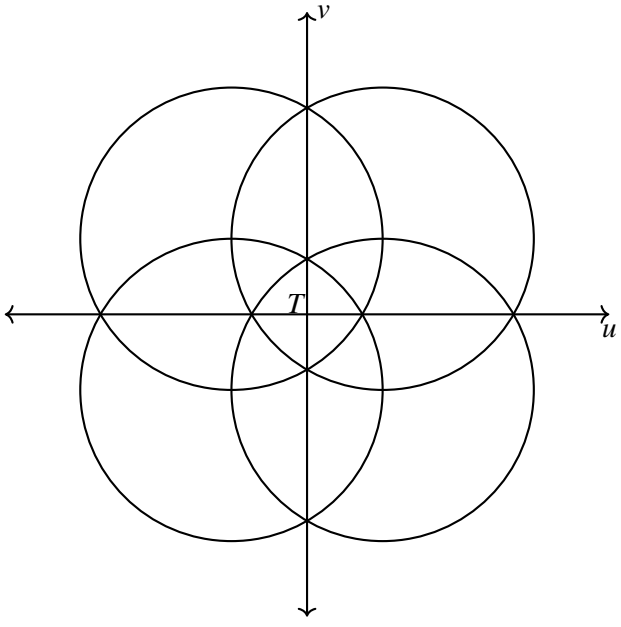

Figure 2.2 The region T we are focusing on in u, v coordinates.

Near a binary collision point interior to T (for example near $q_1 = q_2$ in a region $0 < -u << 1$ and $v, -w \geq \delta > 0$) the metric takes the form

$$(\frac{1}{2u^2} + O(1))(du^2 + dv^2). \tag{2.9}$$

Near the simultaneous binary collision, i.e. in the region $0 < -u, v << 1$, through the change of variable $u + iv = z \mapsto z^2$, the metric takes the same form as eq. 2.9.

Fix our attention on unit speed geodesics and note that by eq. 2.9 above if a geodesic γ passes sufficiently close to the boundary it behaves as a geodesic in the hyperbolic plane – for instance $\alpha(\gamma) \cap \partial T$ must be a point (see figure 2.3).

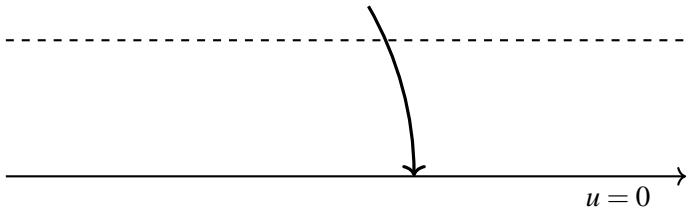

Figure 2.3 Sufficiently near the boundary geodesics behave as in the upper half plane.

Now fix some $q \in \partial T \setminus \{$ triple collisions$\}$ and $p \in \partial T \setminus \{q\}$. We first show the existence of a geodesic from p to q.

Near q (by eq. 2.9), we have that every geodesic γ with $\omega(\gamma)$ sufficiently near p and $\alpha(\gamma)$ near q intersects some compact set I, see figure 2.4.

Next take a sequence of points $q_i \in T^o$ with $q_i \to q$ and a sequence of points $p_i \in T^o$ with $p_i \to p$. Let γ_i be the unique geodesic from p_i to q_i. Then for i large enough all such geodesics intersect I in some point $x_i = \gamma_i(t_i)$. Let $v_i = \dot{\gamma}_i(t_i)$. Now due to the compactness, $(x_i, v_i) \to (x, v) \in I \times \mathbb{R}^2$ and the geodesic $\gamma_{(x,v)}$ goes from p to q.

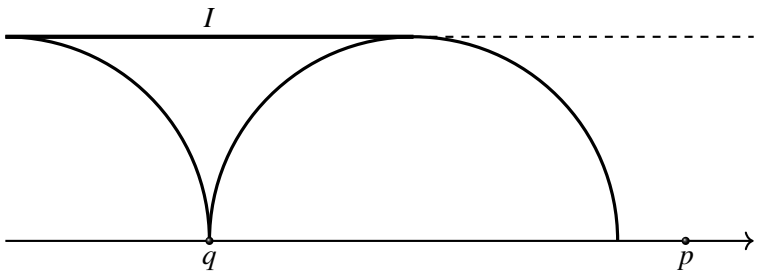

Figure 2.4 The compact set I.

For uniqueness, note that when we have both $p,q \in \partial T \backslash \{$ triple collisions $\}$ then the angles at the boundary between any two geodesics from p to q are zero. So if there were two such geodesics bounding a region R, the Gauss-Bonnet theorem yields

$$2\pi = \int_R K\, dA + \int_{\partial R} \kappa_g\, ds = \int_R K dA + \pi + \pi,$$

which is impossible by the negative curvature (proposition 1). Hence in this case such a geodesic is unique. □

REMARKS: Due to the covering of the exponential map, every geodesic passes sufficiently close to the boundary and hence is characterized uniquely by the points $\alpha(\gamma), \omega(\gamma)$ (except possibly for geodesics beginning or ending in triple collision). The dynamics here on this collinear problem are an attractive case of the *integrable* Calogero-Moser system. In [38] we also observe dynamical consequences from our curvature computations in the parallelogram 4-body problem. The parallelogram problem is an invariant 'shirt', or sphere with 4 punctures. As a consequence of the negative curvature, every tied class on this shirt is realized by a unique periodic solution.

QUESTION: Is there a unique collinear solution connecting two triple collisions? A binary collision to a triple collision?

Chapter 3

Newtonian Force

Here we will examine the syzygy sequences of some orbits arising out of perturbation methods in the planar 3-body problem that were established by Féjoz in [25, 26]. We begin by setting up the unperturbed first approximations or *main problems* ([50], §7.1) we will study. In this section we use notations and computations from appendix A for our Kepler problem coordinates and perturbation expansions.

3.1 The main problems

Let $q_i \in \mathbb{C}, i = 0,1,2$ represent the position of the bodies of mass μ_i, and $p_i = \mu_i \dot{q}_i$ their momenta. The three-body problem flow is the Hamiltonian flow of

$$H = \sum_{i=0}^{2} \frac{|p_i|^2}{2\mu_i} - \sum_{i<j} \frac{\mu_i \mu_j}{|q_i - q_j|}$$

on $T^*(\mathbb{C}^3\backslash\Delta)$ with $\omega = \Re(\sum dp_i \wedge d\overline{q}_i)$. In the symplectic Jacobi coordinates (see appendix A) with the center of mass zero, we may write $H = H_{Kep} + H_{per}$ where

$$H_{Kep} = \sum_{i=1}^{2} \frac{|P_i|^2}{2m_i} - \frac{m_i M_i}{|Q_i|}$$

is a Hamiltonian for two uncoupled Kepler problems and

$$H_{per} = \frac{m_2 M_2}{|Q_2|} - \frac{\mu_1\mu_2}{|Q_2 - \sigma_0 Q_1|} - \frac{\mu_0\mu_2}{|Q_2 + \sigma_1 Q_1|}$$

is the *perturbing part*. The new mass constants are given by $\frac{1}{m_1} = \frac{1}{\mu_0} + \frac{1}{\mu_1}, \frac{1}{m_2} = \frac{1}{\mu_0+\mu_1} + \frac{1}{\mu_2}$ and $M_1 = \mu_0 + \mu_1, M_2 = \mu_0 + \mu_1 + \mu_2$.

In order to justify its name we impose some conditions from [25] on our configurations so that the perturbing part will be small. The condition $|Q_2| > \max\{\sigma_i\}|Q_1|$ prevents the perturbing part from blowing up, and can be ensured by taking initial conditions leading to nested osculating ellipses mod rotations: $a_1(1+e_1) < a_2(1-e_2)$. We are considering here q_2 as the *outer body*, which we will always take to be rotating counterclockwise around the center of mass of the q_0, q_1 system. Note that for the ellipses to not intersect we must exclude a collision outer ellipse, which we do by imposing the condition $e_2 \leq e_2^M < 1$ for some constant e_2^M. Finally the condition

$$\mu a = \frac{(m_1+\mu_2)M_2}{M_1^2}\frac{a_1}{a_2} < \varepsilon$$

ensures the perturbing part is uniformly ε-small, where we take $\mu = \frac{(m_1+\mu_2)M_2}{M_1^2}$ and $a = \frac{a_1}{a_2} < \frac{1}{2}$. The parameter a is small in the *lunar region* where the outer body is distant while the parameter μ is small exactly in the *planetary region* where μ_2 and one of the inner masses are small. The region of configurations satisfying the above conditions is called the *perturbing region*.

By taking symplectic action-angle coordinates (Delaunay or Poincaré, see appendix A) for the Kepler problems, one has the 'fast' angles λ_i, where $i = 1,2$ for the inner or outer Kepler problem with corresponding actions Λ_i. How does the perturbing part disturb this situation?

As the syzygies occur over time scales in the fast variables, λ_i, H_{Kep} will still serve usefully for analyzing the syzygy sequences. However $H_{Kep}(\Lambda_1, \Lambda_2)$ does not take account of how the ellipses slowly deform and as it depends on only two of the three actions is too degenerate to continue solutions. To see how the orbits behave when their mutual attractions are taken into account we will use the study of the *secular dynamics* (from siécle=century) by Féjoz [26]. The main approximation for the secular dynamics is the averaged Hamiltonian:

$$\langle H \rangle = H_{Kep} + \langle H_{per} \rangle,$$

where $\langle H_{per} \rangle := \frac{1}{(2\pi)^2} \int_{T^2} H_{per}\, d\lambda_1 d\lambda_2$. These secular averaged terms are those which cannot be annihilated through symplectic flows of auxiliary Hamiltonians.

In the lunar region, H_{per} has an expansion in powers of a, which renders a representation of this secular dynamics by averaging some of the leading powers in this expansion as carried out in [26]'s appendix.

3.2 Some syzygy sequences of the main problems

As $\varepsilon \to 0$, the deformations of the ellipses from the secular dynamics is much slower than the motions along the ellipses, so it will still be useful to determine the syzygy sequences arising from just H_{Kep}.

Syzygy sequences for two uncoupled Kepler problems:

In Delaunay coordinates, $H_{Kep} = -\frac{m_1^3 M_1^2}{2\Lambda_1^2} - \frac{m_2^3 M_1^2}{2\Lambda_2^2}$ and the flow is a line of slope n_1/n_2 on the mean anomaly (ℓ_2, ℓ_1) torus, where $n_i = \frac{\partial H_{Kep}}{\partial \Lambda_i}$ are the mean motions. The syzygy loci form curves on this torus, and hitting one of these curves results in a certain syzygy. To sketch these curves it is helpful to consider separately the cases of *prograde motion*, when $G_1/G_2 > 0$ and both ellipses are traversed in the same direction, versus *retrograde motion*, when $G_1/G_2 < 0$ and they are traversed in opposite directions.

Consider first the case of retrograde motion and let $g = g_1 - g_2$. As we sweep out the ray of the bodies being alligned (a 1 syzygy) in the direction of increasing ℓ_2 (and so decreasing ℓ_1), we pass from $\ell_1 = 0, \ell_2 = \ell_2(g)$ to $\ell_1 = -2\pi, \ell_2 = \ell_2(g) + 2\pi$ and so oscillate around the line

$$\ell_2(g) = \ell_2 + \ell_1$$

(see figure 3.1). Likewise, when sweeping out the ray of the bodies being in opposition (a 0 syzygy) we oscillate around the line

$$\ell_2(g) + \pi = \ell_2 + \ell_1.$$

Similarly, for prograde motion the 1 syzygy locus oscillates around the line $\ell_2(g) = \ell_2 - \ell_1$ and the 0 locus around the line $\ell_2(g) + \pi = \ell_2 - \ell_1$.

Proposition 3.1. *Consider two nested Keplerian ellipses with eccentricities $e_i \in [0, 1)$. Then*

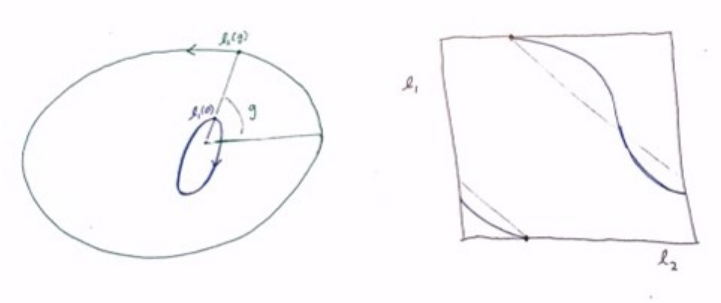

Figure 3.1 Sweeping out a '1' syzygy ray with retrograde motion (the inner ellipse is say more eccentric than the outer ellipse). On the right is the corresponding curve on the (ℓ_2, ℓ_1) torus.

the uncoupled Keplerian flow has a syzygy sequence of the form

$$...1^{a_{-1}}0^{b_{-1}}1^{a_0}0^{b_0}1^{a_1}0^{b_1}...$$

If the motion is prograde the sequence of exponents a_i, b_i may be determined by rotation maps (eqs. 3.2, 3.3), while if the motion is retrograde we have $a_i = b_i = 1$. In the special case that $n_1/n_2 = 1$ and the motion is prograde, the syzygy sequence is either empty or consists of a single symbol.

Proof: The prograde $n_1/n_2 = 1$ case is clear: we either miss the loci entirely or repeatedly intersect one of them. Suppose in the prograde case that $n_1/n_2 > 1$. The syzygy sequence will then alternate between hitting the 0 locus and the 1 locus, and it remains to describe the stutters via the sequences a_i, b_i of exponents.

Stutters occur when it is possible for the flow line to be tangent to these syzygy loci. To compute the slope of the syzygy loci, first note that in polar coordinates, the syzygy loci are given by $\theta_1 = \theta_2$ or $\theta_1 = \theta_2 + \pi$. Now by $d\theta_i = \frac{G_i}{m_i r_i^2} dt = \frac{G_i}{m_i r_i^2 n_i} d\ell_i$ we have that the slope $1 = \frac{d\theta_1}{d\theta_2}$

along the syzygy loci is transformed to

$$\frac{d\ell_1}{d\ell_2} = \frac{m_1 G_2 |Q_1|^2}{m_2 G_1 |Q_2|^2} \frac{n_1}{n_2}.$$

When the motion is retrograde then, since the syzygy loci have negative slope and the flow has positive slope, we alternate between the two symbols 0 and 1, i.e. $a_i = b_i = 1$.

To analyze the syzygies for prograde motion, we 'project the tangencies'. Tangencies of the flow line to the syzygy locus occur when $\frac{n_1}{n_2} = \frac{m_1 G_2 |Q_1|^2}{m_2 G_1 |Q_2|^2} \frac{n_1}{n_2}$, which is at the intersection of the ellipses:

$$r = \alpha_1 x + \beta_1 y + \gamma_1, \;\; r = \alpha' x + \beta' y + \gamma',$$

where $\alpha' = \sqrt{\frac{m_2 G_1}{m_1 G_2}}\alpha_2, \beta' = \sqrt{\frac{m_2 G_1}{m_1 G_2}}\beta_2, \gamma' = \sqrt{\frac{m_2 G_1}{m_1 G_2}}\gamma_2$. In particular, there are either zero, one or two tangencies.

When there are one or zero possible tangencies, then the syzygies alternate between the 0 and 1 syzygy loci as in the retrograde case and hence $a_i = b_i = 1$. The remaining case therefore is when there are two possible tangencies.

Consider the universal cover $\mathbb{R}^2$ of our torus and two consecutive tangency points of the '1' syzygy locus. Project these along the flow lines to the 'base line', which the syzygy loci oscillate around to obtain points $T_1, T_2 \in \{\ell_2(g) = \ell_2 - \ell_1\}$ (see figure 3.2).

The rotation map $R(x) = x + \frac{\pi}{\sqrt{2}} \frac{n_1+n_2}{n_1-n_2} \mod 2\pi\sqrt{2}$ determines where the flow line successively intersects the base line. One may use this map to determine the sequences a_i, b_i as follows.

Let k be the least integer s.t. $|T_1 - T_2| \leq 2\pi\sqrt{2}k$ and $0 \leq \tau_1 \leq \tau_2 < 2\pi\sqrt{2}$ be representatives of T_i measured along the base line $\ell_2(g) = \ell_2 - \ell_1$.

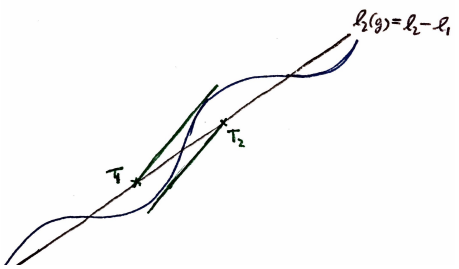

Figure 3.2 Projecting tangencies onto the base line.

We first show by induction that:

$$\text{If } \tau_1 = \tau_2 \text{ then } a_i = 2k+1. \tag{3.2}$$

When $k = 0$ there is one tangency, and we have already seen that here there are no stutters, i.e. $a_i = 1$.

Passing from k to $k+1$ is accomplished by considering figure 3.3.

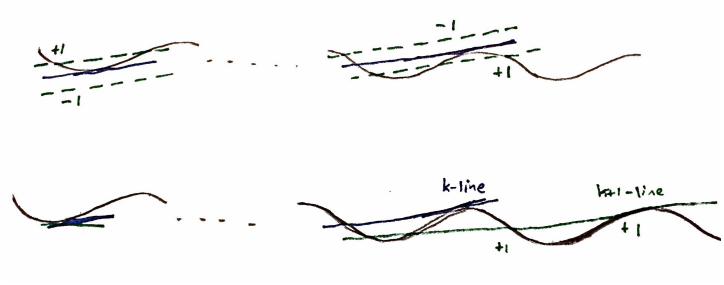

Figure 3.3 When $\tau_1 = \tau_2$, the stutter count is unaffected by a shift (top). Passing from k to $k+1$ increases the intersections by 2 (bottom).

When $\tau_1 \neq \tau_2$, we may shift the $\tau_1 = \tau_2$ case as in figure 3.4 to obtain:

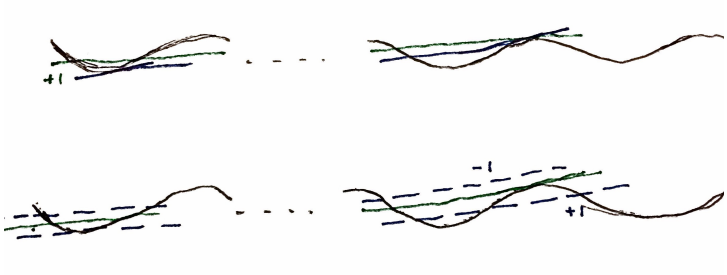

Figure 3.4 At the tangency, passing from $|T_1 - T_2| = 2\pi\sqrt{2}k$ to $|T_1 - T_2| > 2\pi\sqrt{2}k$ adds one stutter from the $\tau_1 = \tau_2$ case. Shifting the flow line to either side increases or decreases the stutter count by one.

$$\text{If } \tau_1 \neq \tau_2 \text{ then } a_i = \begin{cases} 2k+1 & R^i(x_0) \in [0,\tau_1) \cup (\tau_2, 2\pi\sqrt{2}] \\ 2k & R^i(x_0) \in \{\tau_i\} \\ 2k-1 & R^i(x_0) \in (\tau_1, \tau_2) \end{cases}, \tag{3.3}$$

where $x_0 \in [0, 2\pi\sqrt{2})$ is some distance measured along the baseline where the orbit of interest intersects at the initial time. Likewise one may determine the sequence b_i by projecting the '0' tangencies onto the baseline $\ell_2(g) + \pi = \ell_2 - \ell_1$. □

REMARK: Although they are not admitted into the perturbing region, the syzygy sequences for intersecting ellipses can be determined as well by the above method of 'projecting tangencies' and using a rotation map; one just needs to divide the baseline into more subintervals.

Some secular syzygy sequences:

The secular dynamics are that of $\langle H \rangle = \frac{1}{(2\pi)^2} \int_{T^2} H d\ell_1 d\ell_2$. As the fast angles ℓ_i have been averaged out, the secular dynamics take place on the space of ellipses with fixed semi-major axes and a common focus. The system is integrable, having the additional integral $G = G_1 + G_2$. Fixing Λ_i and G and modding by rotations, we have a Hamiltonian flow on a sphere. This sphere has symplectic Delaunay coordinates $G_1, g = g_1 - g_2$ away from the poles. It can be parametrized in non-symplectic spherical coordinates as $(e_1 \cos g, e_1 \sin g, \varepsilon_1)$, where $e_1 = \sin\phi_1, \varepsilon_1 = \cos\phi_1$ for $\phi \in [0, \pi]$. These secular dynamics in the perturbing region are described in [26] (see figure 3.5).

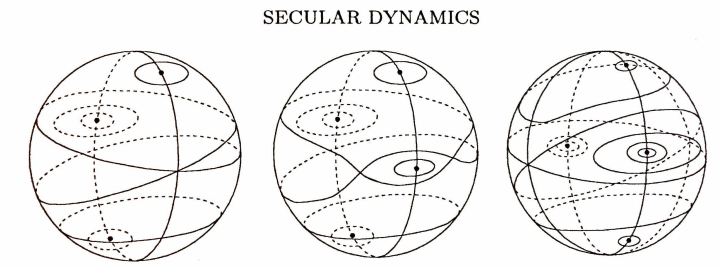

Figure 3.5 This figure from [26] shows a few cases of the singular points of the secular dynamics on the $(e_1 \cos g, e_1 \sin g, \varepsilon_1)$-parametrized sphere. The equator corresponds to collision inner ellipses dividing the sphere into upper and lower hemispheres of prograde or retrograde motion.

We will focus in what follows on the lunar region, by letting $a = \frac{a_1}{a_2} \to 0$ to enter the perturbing region. Because the slow secular variables change only after the inner ellipse has completed many orbits, the syzygy sequences we have found for uncoupled Kepler problems are preserved provided we stay far from the tangencies to the syzygy locus.

Proposition 3.4. *In the lunar region tangencies are possible only when the inner ellipse is oriented prograde and near a degenerate collision ellipse. Angular momentum zero is possible only when the outer mass or the outer and one inner mass are small.*

Proof: The condition for tangencies $\frac{\dot{\ell}_1}{\dot{\ell}_2} = \frac{m_1 G_2 |Q_1|^2}{m_2 G_1 |Q_2|^2} \frac{n_1}{n_2}$ can be written as

$$1 + O(a) = a^{3/2} \sqrt{\frac{M_2}{M_1}} \frac{(1+e_2\cos f_2)^2 (1-e_1^2)^{3/2}}{(1+e_1\cos f_1)^2 (1-e_2^2)^{3/2}},$$

where the $O(a)$ term comes from the secular dynamics. Recall that we have bounded the outer eccentricity above, $e_2 \leq e_2^M < 1$, from which it follows that

$$1 \leq Cst. \sqrt{\frac{M_2}{M_1}} \frac{a^{3/2}}{\sqrt{1-e_1}},$$

where $Cst.$ is a constant depending on e_2^M.

Normalize the masses so that $M_2 = \mu_0 + \mu_1 + \mu_2 = 1$, and suppose that $1 - e_1 = O(a^k)$ and $M_1 = O(a^m)$ for some $k, m \geq 0$ with $k + m = 3$. If we wish to remain in the perturbing region as $a \to 0$, then we must have $a \frac{\mu_0\mu_1 + \mu_2 M_1}{M_1^3} \to 0$ as $a \to 0$, which only holds if $m < \frac{1}{2}$. Hence the only way to satisfy the tangency condition and remain in the lunar regime is when $e_1 = 1 - O(a^k)$ for some $k \in (\frac{5}{2}, 3]$.

Imposing angular momentum zero and staying in the perturbing region (where $e_2 \leq e_2^M < 1$) forces us to remain in the retrograde hemisphere of figure 3.5. In particular we will be far from stutters if the orbit remains in the perturbing region. In fact we may rewrite $G_1 + G_2 = 0$ as

$$a \geq Cst. \frac{\mu_2^2 M_1^2}{\mu_0^2 \mu_1^2 (1-e_1)},$$

where $Cst.$ depends on e_2^M. It follows that angular momentum remains possible in the lunar regions provided we take $\mu_2 = O(a^{m/2}), \mu_0 = O(a^{\ell/2}), e_1 = 1 - O(a^k)$ with $k, \ell, m \geq 0$ and

$m-\ell-k \geq 1$. □

To analyze the syzygy sequences for orbits passing near inner collisions, we use the Levi-Civita regularization.

Proposition 3.5. *If a near inner collision orbit of the secular dynamics has* $e_1 = 1 - O(a^k)$ *and* $k \notin (\frac{5}{2}, 3]$*, then it has a syzygy sequence of the form*

$$...(10)^{a_0}(01)^{a_1}(10)^{a_2}...,$$

where $a_i \in \mathbb{N}$ *are* $O(a^{-3})$.

Proof: Levi-Civita regularize the inner body (appendix 3.3). Then we have $Q_1 = z^2$, where z solves a Harmonic oscillator. By shifting the origin of the regularized time, τ, we may write

$$z = a\cos(b\tau) + ic\cos(b\tau + d),$$

for some constants a, c, d and $b = \frac{\sqrt{M_1}}{2\sqrt{a_1}}$. Let $\theta_i = \arg(Q_i)$.

A '1' syzygy occurs when we have $\theta_1 = \theta_2$, i.e.

$$\tan\frac{\theta_2}{2} = \frac{c\cos(b\tau + d)}{a\cos(b\tau)},$$

while a '0' syzygy occurs when

$$\tan\frac{\theta_2 + \pi}{2} = \frac{c\cos(b\tau + d)}{a\cos(b\tau)}.$$

In figure 3.6 we sketch the syzygy curves for small G_1-values on the torus coordinatized by $(\theta_2, b\tau)$. The flow line on these tori is not straight, but tangent to the direction field

$\frac{d\theta_2}{bd\tau} = \frac{r_1 C_2}{br_2^2}$. In the lunar regions this solution curve is then increasing, but very slowly: $\frac{d\theta}{bd\tau}$ is on the order of $O(a^{3/2})$.

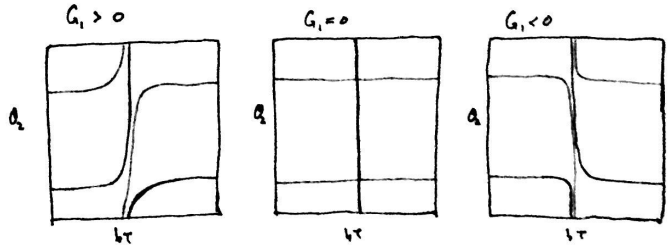

Figure 3.6 The syzygy loci on the regularized $(\theta_2, b\tau)$ tori for different values of G_1. We sketch for values of $b\tau \in [0,\pi]$ as the picture is identical (double cover) for $\tau \in [\pi, 2\pi]$. When $G_1 = 0$ the inner collisions occur along the vertical line $b\tau = \pi/2$.

Note that when $G_1 \neq 0$ we may determine the syzygy sequences without Levi-Civita regularization by proposition 3.1. Namely during prograde motion there are at most two tangency points of the flow to the syzygy curves, and we only pick up an even number of syzygies of a certain type by hitting these tangency points.

Now we consider the syzygy sequence of a near inner collision orbits (see [25, 26]). The secular dynamics of such an orbit are that it switches between prograde motion and retrograde motion (figure 3.7). We also sketch the syzygy loci on the torus $T^3 = (\theta_2, b\tau, g)$ where the full orbit flows in figure 3.7.

This secular system is integrable, and the loci of collision curves and tangencies to the syzygy curves is one dimensional. Hence it is always possible to choose initial conditions to avoid this set, and one obtains a syzygy sequence of the form

$$...(1^{n_0}0^{m_0})^{a_0}(01)^{a_1}(1^{n_1}0^{m_0})^{a_2}(01)^{a_2}...,$$

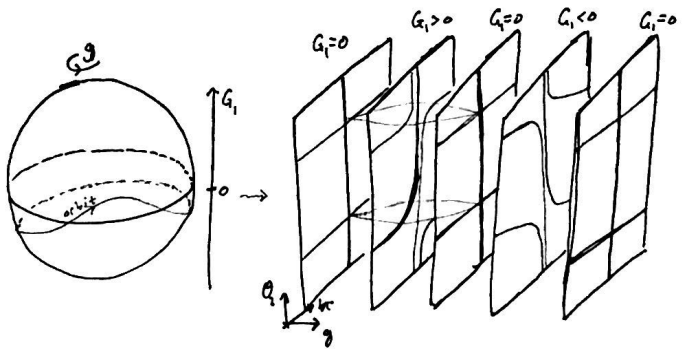

Figure 3.7 On the left is an inner collision secular orbit (G_1 and g's slow change) drawn on a sphere whose height is like G_1 and equatorial angle is like g. On the right are some sections of the $(\theta_2, b\tau, g)$ torus over the secular dynamics with the syzygy curves depicted.

where the n_i, m_i are odd (avoiding the tangencies) and determined as in proposition 3.1 over the prograde part of the motion. As the n_i, m_i are odd, by cancelling their stutters we find a syzygy sequence of the form

$$...(10)^{a_0}(01)^{a_1}(10)^{a_2}...,$$

where the a_i occur on the time scale $(\frac{dg}{dt})^{-1}$, which is $O(a^{-3})$.

Finally, recalling the proof of proposition 3.4, provided one chooses $e_1 = 1 - O(a^k)$ for $k \notin (\frac{5}{2}, 3]$ there will be no prograde tangencies and thus no stutters. In this case the *true* syzygy sequence will be of the form $...(10)^{a_0}(01)^{a_1}...$ Furthermore these orbits are 'far from tangencies' in the sense that the orbit always intersects the syzygy locus at an angle bounded below by a *fixed* constant. □

3.3 Some syzygy sequences in the lunar regions

In this section we will verify some non-degeneracy conditions, which allow the secular orbits in the lunar regions to be continued to the full 3-body problem. These arguments are well known (cf. [25, 28]). The only contribution here is the description of these orbits by their syzygy sequences. Having verified in the previous section certain cases when the unperturbed orbits are far from tangencies to the syzygy loci, we may conclude that these continued solutions, which remain in the perturbing region, retain the same syzygy sequences of §3.2 establishing theorem 4.

Quasi-periodic orbits:

We will apply a KAM theorem in order to continue quasi-periodic, angular momentum zero orbits over the fixed point of the secular dynamics near a circular inner ellipse (near a pole on the secular dynamics sphere of figure 3.5).

To state this theorem, let us recall that a vector $\alpha \in \mathbb{R}^n$ is called *Diophantine* if there exist constants $\gamma, \tau > 0$ s.t. for every $k \in \mathbb{Z}^n \backslash 0$, we have

$$|\alpha \cdot k| \geq \frac{\gamma}{|k|^\tau}.$$

We write $D_{\gamma,\tau}$ for the set of all such vectors with the constants γ, τ (see figure 3.8). Also we let $(r, \theta) \in \mathbb{R}^n \times T^n$ be conjugate coordinates and B^k be the unit ball in $\mathbb{R}^k$.

Theorem 5. *[28]. Fix $\gamma > 0$ and $\tau \geq n-1$. Consider an analytic family of Hamiltonians of the*

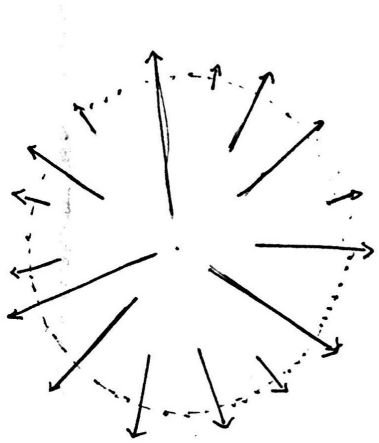

Figure 3.8 A depiction of the set $D_{\gamma,\tau}$ in $\mathbb{R}^2$. Note that if $\alpha \in D_{\gamma,\tau}$ then so is $\lambda\alpha$ for $\lambda \geq 1$. $D_{\gamma,\tau}$ forms a 'transversally Cantor set' that is like $C \times \mathbb{R}_+$, where C is the Cantor set.

form

$$F_s^o = c_s^o + \alpha_s^o \cdot r + O(r^2; \theta),$$

where $s \in B^k$ are the parameters of the family and $c_s^o \in \mathbb{R}, \alpha_s^o \in \mathbb{R}^n$. If $\alpha_0^o \in D_{\gamma,\tau}$ then there exists a constant $Cst. > 0$ (depending on τ and the analycity width of F_s^o) such that whenever a family of analytic Hamiltonians F_s satisfies

$$|F_s - F_s^o|_{B^k} \leq Cst.\gamma^2$$

then it follows that:

(i) *There exists a map $B^k \to \mathbb{R}^n, s \mapsto \alpha_s$ with $|\alpha_s - \alpha_s^o| << 1$.*

(ii) *Whenever $\alpha_s \in D_{\gamma,\tau}$, then $F_s = c_s + \alpha_s \cdot r + O(r^2; \theta)$ (i.e. F_s has an invariant torus).*

REMARKS: The criteria $\alpha_s \in D_{\gamma,\tau}$ of (ii) may be vacuous! It is to ensure the hypotheses of (ii) hold that one imposes some non-degeneracy assumptions on α_s^o so that (i) implies

that condition (ii) is not vacuous. Two such non-degeneracy conditions are illustrated in figure 3.9.

It is not necessary that α^o be Diophantine at the center of the ball, but rather it suffices to know $\alpha^o_{s_0} \in D_{\gamma,\tau}$ for some $s_0 \in B^k$. Moreover the parameters s may vary only over some open set that is topologically B^k provided the estimates hold uniformly over this open set.

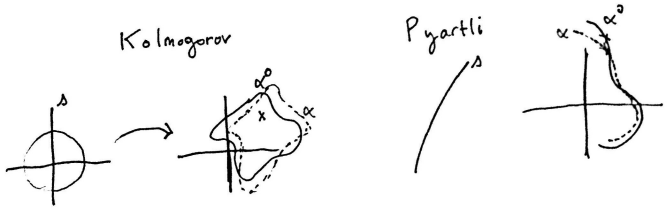

Figure 3.9 The Kolmogorov nondegeneracy condition is that $s \mapsto \alpha^o_s$ is a diffeomorphism. In this case α near α^o implies we also find Diophantine frequencies for α. The Pyartli condition is that α^o should be a skew map: its image is not contained in any hyperplane. This condition also ensures that sufficiently close α will have some Diophantine frequencies as well (see figure 3.8).

Our task in applying theorem 5 to the Kepler problem is first to determine what to take for F^o_s and F_s. To do this let us recall from the appendix 3.3 the expansion

$$H = H_{Kep} + H_{Quad} + O(\varepsilon^4),$$

where $a_1/a_2 \sim \varepsilon$ since we are exploring the lunar regions. In the 'polar Poincaré' variables and with angular momentum $C = 0$ we have (see appendix §3.3 eq. 3.7)

$$H_{Quad} = c_1 + \alpha_1 \rho_1 + O(\rho_1^2),$$

where $c_1 = c_m \frac{\Lambda_1}{\Lambda_2^3}$ and $\alpha_1 = \alpha_m \frac{1}{\Lambda_2^3}$ for some constants c_m, α_m depending on the masses.

If we set $r = (\Lambda_i - \Lambda_i^o, \rho_1)$ and take F_s^o as the Taylor expansion of $H_{Kep} + H_{Quad}$ around $\Lambda_i = \Lambda_i^o, \rho_1 = 0$, we have

$$F_s^o = c_s^o + \alpha_s^o \cdot r + O(r^2),$$

for $c_s^o = H_{Kep}(\Lambda_i^o) + c_1(\Lambda_i^o)$ and $\alpha_s^o = (n_1^o + c_m \frac{1}{(\Lambda_2^o)^3}, n_2^o - 3c_m \frac{\Lambda_1^o}{(\Lambda_2^o)^4}, \alpha_m \frac{1}{(\Lambda_2^o)^3})$. By taking $s = (u,v) = (\frac{1}{\Lambda_1^o}, \frac{1}{\Lambda_2^o})$ as our parameters we have

$$\alpha_s^o = (au^3 + bv^3, v^3(c + dv/u), ev^3),$$

where a, b, c, d, e are some mass constants. Taking an expansion of H in the same parameters for F_s, we have $|F_s - F_s^o| = O(\varepsilon^4)$.

The next item to take care of is that α_s^o satisfies a non-degeneracy condition. We will check the 'Pyartli condition', that the frequency map is skew for angular momentum zero. This is equivalent to (see [28] §7) the non-vanishing of

$$\det[\partial_u^2 \alpha_s^o \;\; \partial_{uv}^2 \alpha_s^o \;\; \partial_v^2 \alpha_s^o].$$

A quick computation gives this determinant as $adev^4/u \neq 0$, so indeed the frequency map is skew.

Finally, although it is tempting to fix γ, τ and let $\varepsilon \to 0$, this may be problematic because the frequency α_s^o depends on ε. Namely, we have

$$\alpha_s^o = O(1, \varepsilon^{3/2}, \varepsilon^{3/2}).$$

There is a Lemma of Rüssman ([28] pg. 24) that states that the measure of $\{s : \alpha_s^o \notin D_{\gamma,\tau}\}$

is $O((\gamma/\varepsilon^{3/2})^{1/\mu})$ for some $\mu > 0$. Hence as $\varepsilon \to 0$ we have no way to ensure that there exist $\alpha_s^o \in D_{\gamma,\tau}$ for a fixed γ, τ!

We may circumvent this issue by scaling γ since we know that the closeness required in theorem 5 is $O(\gamma^2)$. Hence take $\gamma = \varepsilon^m \bar{\gamma}$ and fix $\tau > n-1$. Then the closeness required for theorem 5 is $O(\varepsilon^{2m})$, while Rüssman's Lemma implies that the measure of $\{s : \alpha_s^o \notin D_{\gamma,\tau}\}$ is $O(\varepsilon^{(m-3/2)/\mu})$. Recalling our Legendre polynomial expansion has shown that $|F_s - F_s^o| = O(\varepsilon^4)$, we can see a nice choice of m is between $3/2$ and 2.

In summary, if we take $m \in (3/2, 2)$, then as $\varepsilon \to 0$, we find that the closeness of the three body problem to the approximation $H_{Kep} + H_{Quad}$ becomes sufficient to apply theorem 5 (since $O(\varepsilon^4) < O(\varepsilon^{2m})$). Finally, the skew condition has been verified and by Rüssman's Lemma there are some frequencies of $\alpha_s^o \in D_{\gamma,\tau}$ (the measure of their complement nearby such frequencies is $O(\varepsilon^{(m-3/2)/\mu})$ and goes to zero). Again by the skew condition and the fact that α_s is near α_s^o, there are some frequencies of $\alpha_s \in D_{\gamma,\tau}$, so that condition (ii) of theorem 5 is not vacuous!

Periodic orbits:

Here we apply an implicit function theorem argument similar to that in Poincaré [63] §42 to continue periodic orbits over fixed points of the secular dynamics. This 'averaging approach' is also described in [57, 65].

Let us begin with the scaled coordinates of Féjoz ([25] pg. 10), defined by choosing a Λ_0 such that in the limit as $\varepsilon \to 0$ one has $\frac{\min\{\Lambda_i\}}{\Lambda_0} \in (0, \infty)$. The rescaled coordinates are

$\Lambda_j = \Lambda_0\tilde{\Lambda}_j, \xi_j = \sqrt{\Lambda_0}\tilde{\xi}_j, \eta_j = \sqrt{\Lambda_0}\tilde{\eta}_j, \lambda_j = \tilde{\lambda}_j$, which by abuse of notation we continue to write without the twiddle's. We will write the rescaled Hamiltonian as $F = H/\Lambda_0$. Now fix the angular momentum C. Féjoz has shown that this rescaled Hamiltonian has an expansion over the asynchronous region (contained inside the lunar region) as:

$$F = F_{Kep}(\Lambda_i) + \langle F \rangle(\Lambda_i, \xi_1, \eta_1) + F_{comp}(\Lambda_i, \lambda_i, \xi_1, \eta_1),$$

where F_{Kep} is a Hamiltonian for two uncoupled Kepler problems and $\langle F \rangle = O(\varepsilon)$ is the average of F over the fast λ_i variables and $F_{comp} = O(\varepsilon^2)$.

Consider a periodic orbit of F when $\varepsilon = 0$, i.e. an orbit of F_{Kep} and initial conditions Λ_i^o yielding *resonant* frequencies:

$$k_1 n_1^o + k_2 n_2^o = 0,$$

for some $(k_1, k_2) \in \mathbb{Z}^2 \backslash 0$. We will take ξ_1^o, η_1^o to correspond to the fixed point of the secular dynamics near the inner circular ellipse.

To continue this orbit we will examine a first return or Poincaré map in the following *flow straightening* coordinates. Since k_1, k_2 may be chosen relatively prime, there exist $h_1, h_2 \in \mathbb{Z}\backslash 0$ s.t. $k_1 h_2 - k_2 h_1 = 1$. That is to say

$$\varphi = \begin{bmatrix} \varphi_1 \\ \varphi_2 \end{bmatrix} = \begin{bmatrix} k_1 & k_2 \\ h_1 & h_2 \end{bmatrix} \begin{bmatrix} \lambda_1 \\ \lambda_2 \end{bmatrix} = M\lambda$$

defines a map from $(\mathbb{R}/2\pi\mathbb{Z})^2$ to itself. Take

$$M^t J = \Lambda - \Lambda^o$$

as the translated symplectic lift (so that $J = 0$ corresponds to Λ^o).

The equations of motion for F_{Kep} are then

$$\dot{J} = 0, \;\; \dot{\varphi} = \omega(J) = \begin{bmatrix} \omega_1 \\ \omega_2 \end{bmatrix} = \begin{bmatrix} \alpha^o J_1 + \gamma^o J_2 \\ \omega_2^o + \beta^o J_2 + \gamma^o J_1 \end{bmatrix} + O(J^2), \tag{3.6}$$

where $\alpha^o = -\frac{n_1^o k_1^2}{\Lambda_1^o} - \frac{n_2^o k_2^2}{\Lambda_2^o} \neq 0$. In particular our periodic orbit of F_{Kep} has been 'straightened' into an orbit of period $2\pi/\omega_2^o$ given by:

$$J = 0, \; \varphi_1 = \varphi_1^o, \; \varphi_2 = \omega_2^o t + \varphi_2^o.$$

Our Poincaré section will be $\varphi_2 = 0$ with Poincaré map P_ε (see figure 3.10). Note that since $\partial_{J_2} F \neq 0$ in a neighborhood of the periodic orbit, the implicit function theorem gives $J_2(J_1, \xi_1, \eta_1, \varphi_i)$ on a fixed energy surface. So by keeping the energy fixed, it suffices to consider the returns of the variables $J_1, \xi_1, \eta_1, \varphi_1$ to the $\varphi_2 = 0$ section.

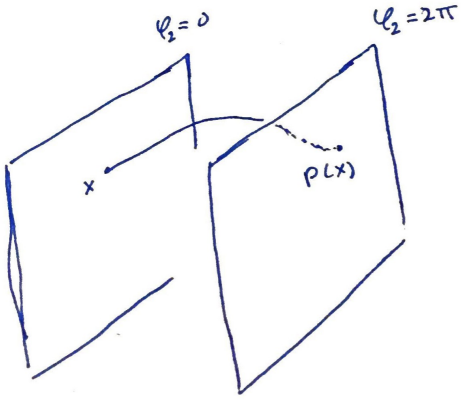

Figure 3.10 The Poincaré return map to the $\varphi_2 = 0$ section.

The goal is now to show that at $\varepsilon = 0$, the map $\psi = P_0 - id$ has a non-degenerate zero, allowing us to continue this root and hence periodic solution for small ε by the implicit function theorem. However when $\varepsilon = 0$ we have $\psi(J_1, \xi_1, \eta_1, \varphi_1) = (0, 0, 0, 2\pi\omega_1/\omega_2)$, which

is very degenerate due to all of J_i, ξ_1, η_1 being constant under the Keplerian flow. We will use the following 'scaling' of Poincaré to see the higher order terms in a modified return map.

Consider J_1; since $\dot{J}_1 = -\partial_{\varphi_1} F_{comp}$ we have

$$J_1^t - J_1^o = -\partial_{\varphi_1} \int_0^t F_{comp}(J_1^s, J_2(J_1^s, \xi_1^s, \eta_1^s, \varphi_i^s), \xi_1^s, \eta_1^s, \varphi_i^s)\, ds,$$

where $F_{comp} = O(\varepsilon^2)$ and wish to continue zeroes of this map from $\varepsilon = 0$. However it suffices to continue a zero of $\frac{J_1^t - J_1^0}{\varepsilon^2}$, since this is a stronger condition. Hence take $F_2 := F_{comp}/\varepsilon^2$ and send $\varepsilon \to 0$. We arrive at the map

$$J_1 \mapsto -\int_0^{2\pi/\omega_2} \partial_{\varphi_1} F_2(J_1, J_2(J_1), \xi_1, \eta_1, \omega_1 s + \varphi_1, \omega_2 s)\, ds =: -\partial_{\varphi_1} F_{res}(J_1, \xi_1, \eta_1, \varphi_1).$$

Likewise for the other variables in this scaled return map (take $F_1 := \langle F \rangle / \varepsilon$) we have:

$$\varphi_1 \mapsto 2\pi \frac{\omega_1}{\omega_2},$$

$$\xi_1 \mapsto -\partial_{\eta_1} F_1(J_1, \xi_1, \eta_1),$$

$$\eta_1 \mapsto \partial_{\xi_1} F_1(J_1, \xi_1, \eta_1),$$

and call this map $\overline{\psi} = \overline{P}_0 - id$, whose non-degenerate zeroes we seek.

The linearization of $\overline{\psi}$ is:

$$\begin{bmatrix} * & -\partial^2_{\varphi_1} F_{res} & * & * \\ 2\pi \partial_{J_1} \frac{\omega_1}{\omega_2} & 0 & 0 & 0 \\ * & 0 & -\partial_{\xi_1}\partial_{\eta_1} F_1 & -\partial^2_{\eta_1} F_1 \\ * & 0 & \partial^2_{\xi_1} F_1 & \partial_{\eta_1}\partial_{\xi_1} F_1 \end{bmatrix},$$

which mod signs has determinant

$$2\pi\partial_{J_1}(\frac{\omega_1}{\omega_2})\partial^2_{\varphi_1}(F_{res})\det\begin{bmatrix}\partial^2_{\xi_1}F_1 & \partial_{\xi_1}\partial_{\eta_1}F_1\\ \partial_{\xi_1}\partial_{\eta_1}F_1 & \partial^2_{\eta_1}F_1\end{bmatrix}.$$

It remains to verify this expression is non-zero when $J=0$ and ξ_1^o,η_1^o are at the secular fixed point near the circular inner ellipse in order to continue the Keplerian periodic orbit we began this section with.

The dominant term of the secular dynamics is H_{Quad}, and we have $H_{Quad} = c_1 + \frac{\alpha_1}{2}(\xi_1^2+\eta_1^2)+O(\rho_1^2)$, where $\alpha_1 \neq 0$, so that this near inner ellipse critical point (near $\xi_1=\eta_1=0$) is non-degenerate.

Next, by differentiating $cst. = \omega_2^o J_2 + \frac{\alpha^o}{2}J_1^2 + \frac{\beta^o}{2}J_2^2 + \gamma^o J_1 J_2 + ...$ and setting $J_1 = J_2 = 0$ we obtain $\frac{dJ_2}{dJ_1}|_{J=0} = 0$. And so from the expansions eq. 3.6 for ω_i, we have

$$\partial_{J_1}(\frac{\omega_1}{\omega_2})|_{J=0} = \frac{\alpha^o}{\omega_2^o} \neq 0.$$

Finally we need to check that $F_{res}(0,\xi_1^o,\eta_1^o,\varphi_1)$ as a function of $\varphi_1 \in S^1$ has a non-degenerate critical point. We carry out this computation in appendix A. Writing $\approx$ for terms that are equivalent modulo terms not depending on φ_1, we find

$$F_{res}(0,\xi_1^o,\eta_1^o,\varphi_1) \approx \cos(2(h_1+h_2)\varphi_1)+O(e_i),$$

which, since the secular fixed point we are considering is near circular ellipses ($e_i << 1$), is non-degenerate!

In [25] similar averaging arguments as above are carried out with Levi-Civita coordinates, which regularize the inner collision and allow one to continue the periodic and

quasi-periodic orbits that satisfy the requirements of proposition 3.5. Again, as these syzygy sequences occur far from tangencies, the continued solutions will have the same syzygy sequences. Obtaining better estimates on the a_i from proposition 3.5 would be essential in determining whether such near inner-collision solutions unwind themselves to reduce to the empty class.

Appendix A

This appendix contains some mechanics background and the notations used in §3. I mainly follow the nice references [4, 9, 50, 27, 16].

Mechanics

As we learn in physics, force is proportional to mass times acceleration. That is the differential equations of physics are second order:

$$\ddot{x} = F(m, x, \dot{x}, t), \tag{3.1}$$

where m stands for mass constants. Such differential equations do not correspond to vector fields on a configuration space, $X \ni x$, but rather as certain vector fields on the tangent bundle TX.

Indeed, elements of TTX are represented by variations of curves. Let $\gamma_s(t)$ be a family of curves. To this variation we have the curve $(\gamma_s, \frac{d\gamma_s}{dt})$ in TX and the tangent vector $(\gamma_s, \frac{d\gamma_s}{dt}, \frac{d\gamma_s}{ds}, \frac{d^2\gamma_s}{dsdt}) \in TTX$. The acceleration or 2-jet of a curve $x(t) \in X$ can be seen in TTX as

arising from the variation $\gamma_s(t) = x(s+t) = x(\tau)$, which gives

$$(x, \frac{dx}{d\tau}, \frac{dx}{d\tau}, \frac{d^2x}{d\tau^2}) \in TTX.$$

The reference [9] has a nice description of TTX and the relationship between the Lagrangian and Hamiltonian formulations of eq. 3.1.

In this appendix we will take a more concrete approach to describe the parts of the Hamiltonian framework that we use above. Consider the case when eq. 3.1 has the form $\ddot{x} = \frac{\partial U}{\partial x}(x)$ for some potential function $U : X \to \mathbb{R}$. The standard process for converting this second order differential equation into a first order one gives the system

$$\dot{x} = y, \;\; \dot{y} = \frac{\partial U}{\partial x}.$$

The *Hamiltonian form* of these equations consists of taking the energy or *Hamiltonian function*

$$H(x,y) = \frac{1}{2}|y|^2 - U(x),$$

for which we have

$$\dot{x} = \frac{\partial H}{\partial y}, \;\; \dot{y} = -\frac{\partial H}{\partial x}.$$

More cryptically, but compactly, one may consider $H : T^*X \to \mathbb{R}$ as generating the *Hamiltonian vector field* X_H defined by

$$-dH = i_{X_H}\omega, \tag{3.2}$$

where $\omega = d\lambda$ and λ is the *canonical 1-form*[1] on T^*X.

[1] For $\pi : T^*X \to X$ the canonical projection, and $\xi \in T_pT^*X$ take $\lambda_p(\xi) := p(d\pi\xi)$.

EXAMPLE: For $X = \mathbb{R}^n$ we take coordinates $(x,p) \in \mathbb{R}^{2n}$ for $T^*\mathbb{R}^n$. Then $\lambda = p_i dx^i$ and $\omega = dp_i \wedge dx^i$. One computes that $X_H = \sum \frac{\partial H}{\partial p_k}\partial_{x_k} - \frac{\partial H}{\partial x_k}\partial_{p_k}$ and that the matrix expression for ω is $\langle J\cdot,\cdot\rangle$, where $J = \begin{bmatrix} 0 & -I_n \\ I_n & 0 \end{bmatrix}$ and $\langle\cdot,\cdot\rangle$ is the standard Euclidean inner product on $\mathbb{R}^{2n}$.

Now in studying equations of motion under the Hamiltonian framework, we should only consider changing coordinates that preserve the form[1] of eq. 3.2. Such coordinate changes are called *canonical* or *symplectic*.

EXAMPLE: Let us lift the change of variables $\xi = Ax$ on $X = \mathbb{R}^n$ to a symplectic change of variables on T^*X. In order for $\pi = Bp$ to accomplish this we need: $\omega(Cu,Cv) = \omega(u,v)$ for all u,v where $C = \begin{bmatrix} A & 0 \\ 0 & B \end{bmatrix}$. This is equivalent to $C^t JC = J$, which implies $B^{-1} = A^t$. This process is called the *symplectic lift* of A.

The *Lagrange parentheses* and *Poisson brackets* (see [23]) are useful to determine whether a coordinate change will by canonical, and they are defined as follows. Let $\zeta = (\zeta_1,...,\zeta_{2n})$ be some coordinates on T^*X and

$$\omega = \sum_{i<j} \omega_{ij} d\zeta_i \wedge d\zeta_j.$$

Then the Lagrange parentheses are defined as $(\zeta_i,\zeta_j) = \omega_{ij}$ (and $\omega_{ji} = -\omega_{ij}$), so the

[1] Meaning if $(\xi,\pi) = \phi(x,p)$ is a change of coordinates on T^*X then with $H \circ \phi^{-1} =: K$ we have $\dot{\xi} = \frac{\partial K}{\partial \pi}, \dot{\pi} = -\frac{\partial K}{\partial \xi}$. This is equivalent to $\phi^*\omega = \omega$.

differential equations associated to the Hamiltonian flow of H, $\dot{\zeta} = X_H$ take the form:

$$\sum_j (\zeta_j, \zeta_k)\dot{\zeta}_j = i_{\dot{\zeta}}\omega(\partial_{\zeta_k}) = -\frac{\partial H}{\partial \zeta_k},$$

and the change is symplectic when $(\zeta_j, \zeta_{n+k}) = \delta_{jk}, (\zeta_j, \zeta_k) = 0$ for $1 \leq j,k \leq n$.

Likewise we define the Poisson brackets by:

$$\dot{\zeta}_j = \sum_k \{\zeta_j, \zeta_k\}\frac{\partial H}{\partial \zeta_k},$$

and can again see that the change of variables is canonical when $\{\zeta_j, \zeta_{n+k}\} = \delta_{jk}, \{\zeta_j, \zeta_k\} = 0$, for $1 \leq j,k \leq n$.

The Poisson brackets have another nice interpretation. Writing $X_{\zeta_k} = X_k^\ell \partial_{\zeta_\ell}$ we have:

$$\delta_{ij} = d\zeta_i(\partial_{\zeta_j}) = -\omega(X_{\zeta_i}, \partial_{\zeta_j}) = -X_i^\ell \omega_{\ell j},$$

so that $-[X_i^j] = [\omega_{k\ell}]^{-1}$, i.e. $X_i^j = \{\zeta_i, \zeta_j\}$. And now

$$\omega(X_{\zeta_i}, X_{\zeta_j}) = -d\zeta_j(X_i^\ell \partial_{\zeta_\ell}) = X_i^j = \{\zeta_i, \zeta_j\}. \tag{3.3}$$

This eq. (3.3) allows one to see the connection between symmetries and integrals and can be more convenient for computation as we will see next in following Féjoz's exposition [27] of the classic coordinates of celestial mechanics.

Kepler problem

One calls a particle attracted to a fixed center according to Newton's law the Kepler problem. The equation of motion is: $m\ddot{q} = -\frac{mM}{|q|^3}q$, where $q \in \mathbb{C}\backslash 0$. In polar coordinates, $q = re^{i\theta}$, we find the *angular momentum* $G := \Im(\overline{q}p) = mr^2\dot{\theta} = const.$ and $\ddot{r} = \frac{-Mr+G^2}{r^3}$. So there

exists a solution to this equation giving $r(t)$, and as noted by Lagrange (see [23]), the components of $q = x + iy$ are solutions to the homogeneous part of the same differential equation:

$$\ddot{X} = \frac{-MX}{r(t)^3} + \frac{G^2}{r(t)^3}.$$

Hence

$$r = \alpha x + \beta y + G^2/M$$

($r = G^2/M$ being a particular solution) for some constants α, β, which is a conic section. We consider elliptical orbits in what follows.

Take a as the semi-major axis, e as the eccentricity and g as the *argument of pericenter* of this ellipse (figure 3.11) and write this ellipse in polar coordinates as

$$r = \frac{a(1-e^2)}{1+e\cos f},$$

where $f = \theta - g$ is the *true anomaly*.

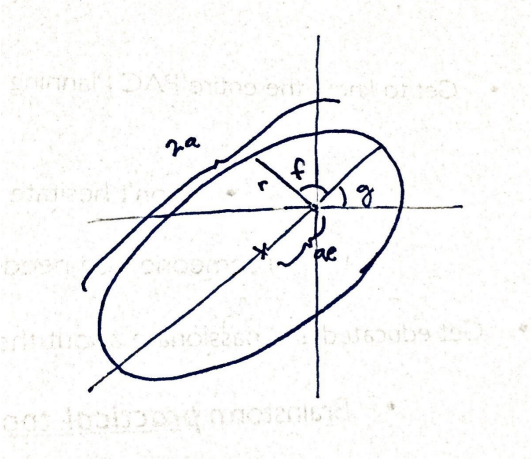

Figure 3.11 An ellipse, ae is the distance from the focus to the center.

In Hamiltonian form we have $H = \frac{|p|^2}{2m} - \frac{mM}{|q|}$, and again in polar coordinates, $H =$

$m\frac{\dot{r}^2}{2} + \frac{G^2}{2mr^2} - \frac{mM}{r}$, so that the extremal values of r (where $\dot{r} = 0$) are roots of the equation $r^2 + \frac{mM}{H}r - \frac{G^2}{2mH} = 0$, which we already know to be $a(1-e)$ and $a(1+e)$. Hence

$$2a = -\frac{mM}{H},\ a(1-e^2) = \frac{G^2}{m^2M}.$$

It remains to express the position on the conic in a nice way. As area is swept at the constant rate $G/2m$, define the *mean anomaly*,

$$\ell := 2\pi\frac{Area(t)}{Area(ellipse)}.$$

Then $\frac{d\ell}{dt} = n$ where $n^2 = \frac{G^2}{m^2a^4(1-e^2)} = Ma^{-3}$ and we choose n to be positive (n is called the *mean motion*, note that the meaning of n for the position on the ellipse depends on the sign of G e.g. $G > 0$ then area swept out counterclockwise is increasing).

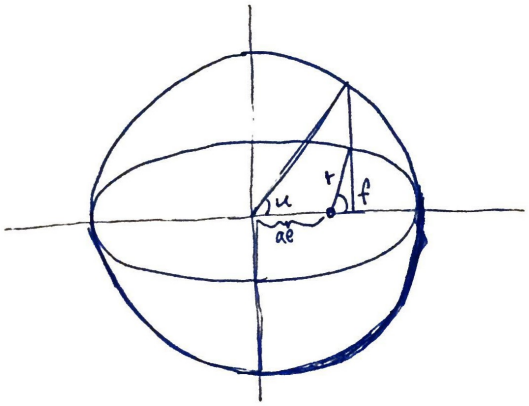

Figure 3.12 The eccentric anomaly is the usual parametrization of the ellipse from the center: $(a\cos u, b\sin u)$ where $b = a\sqrt{1-e^2}$. We have $a\cos u - ae = r\cos f$ and $b\sin u = r\sin f$.

To relate f to ℓ we use the *eccentric anomaly*, u, which is an angle defined $\mod 2\pi$ by parametrizing from the center of the ellipse as $(a\cos u, a\sqrt{1-e^2}\sin u)$ and so relates to f by figure 3.12. To relate u to ℓ we compute area using Stoke's formula: the area swept out by the

curve $(a\cos u - ae, b\sin u)$ is

$$\frac{1}{2}\int_0^u xdy - ydx = \frac{ab}{2}(u - e\sin u),$$

which compared with the defining equation for ℓ gives

$$\ell = u - e\sin u.$$

Hence to define position on the ellipse in terms of time one finds u in terms of ℓ and then f in terms of u through $\tan\frac{f}{2} = \sqrt{\frac{1+e}{1-e}}\tan\frac{u}{2}$.

The goal is to have some geometric coordinates for the positions of the bodies that also preserve the canonical form of the equations. For eccentricities $e \in (0,1)$ the *Delaunay coordinates* do this trick.

Since ℓ is already so nice, we seek a variable $\Lambda(H)$ conjugate to it, i.e. $d\Lambda \wedge d\ell = dH \wedge dt$ or $\frac{d\Lambda}{dH} = n^{-1}$, which yields, according to the formulas above,

$$\Lambda^2 = -\frac{m^3M^2}{2H},$$

and we choose Λ to be positive. Now the Delaunay coordinates are

$$(\Lambda, G, \ell, g)$$

which are canonical. This can be computed nicely via the Poisson brackets, as done by Féjoz in [27]: $\{\Lambda,\ell\} = 1$ by definition, and $\{\Lambda, G\} = 0, \{\Lambda, g\} = 0$ since G, g are constants under the Hamiltonian flow of H (or $\Lambda(H)$); $\{G, g\} = 1$ since g is an angle and the Hamiltonian flow of G is just rotation. Also $\{G,\ell\} = 0$ since rotating an ellipse does not change position on the ellipse. Finally, we show $\{g,\ell\} = 0$. Jacobi's identity yields $\{\cdot, \{g,\ell\}\} = 0$ and, in particular, $\{g,\ell\}$ is

constant under the Hamiltonian flow of G and Λ. Under these flows any point always passes through $g = 0, \ell = 0$ (we can rotate the ellipse so that $g = 0$ under the flow of G and then move along the ellipse under the flow of Λ until we are at pericenter). At such a point, $g_x = 0, \ell_x = 0$ and $g_{p_y}, \ell_{p_y} = 0$, since varying x or p_y just changes the size of the ellipse but does not move the pericenter direction. Hence:

$$\{g, \ell\} = g_x \ell_{p_x} - g_{p_x} \ell_x + g_y \ell_{p_y} - g_{p_y} \ell_y = 0.$$

When $e = 0$ and the orbits are circular the Delaunay coordinates break down, ℓ and g are no longer well defined! In the neighborhood of these regions the *Poincaré coordinates* take care of business (again see [27] for a nice motivation). Take $\lambda = \ell + g$ and $\xi + i\eta = \sqrt{2(\Lambda - |G|)} e^{-ig}$. Then the Poincaré coordinates are

$$(\Lambda, \xi, \lambda, \eta),$$

with 'polar version' as

$$(\Lambda, \rho, \lambda, \phi),$$

where $\rho = \Lambda - |G|, \phi = g$.

Finally, when $e = 1$ we have a collision ellipse and invoke the *Levi-Civita regularization* ([25, 41]). Recall we identify $p \in \mathbb{C}$ with the 1-form $p d\overline{q} + \overline{p} dq$. Then the cotangent lift of the double cover $l(z) = z^2 = q$ is defined by $l^* p = w$ or $w d\overline{z} + \overline{w} dz = 2\overline{z} p d\overline{z} + 2z\overline{p} dz$, that is $p = \frac{w}{2\overline{z}}$ and this is the Levi-Civita map:

$$LC : T^*\mathbb{C}\backslash\{0\} \to T^*\mathbb{C}\backslash\{0\}, (z, w) \mapsto (z^2, \frac{w}{2\overline{z}}) = (q, p).$$

As a cotangent lift, the map is symplectic and for $H = \frac{|p|^2}{2m} - \frac{mM}{|q|}$ we have $LC^*H = \frac{|w|^2}{8m|z|^2} - \frac{mM}{|z|^2}$, so that

$$LC^*|q|(H+h) = \frac{|w|^2}{8m} - mM + h|z|^2$$

is a nice harmonic oscillator (having no problems with $z = 0$). Taking $K = |q|(H+h)$ we have

$$dLC^*K = (dLC^*|q|)LC^*(H+h) + |z|^2 dLC^*H. \tag{3.4}$$

And from equation (3.4) it follows that the Hamiltonian flow of LC^*K on the level set $LC^*K = 0$ and $z \neq 0$ (corresponding to $H = -h$) is just the Kepler flow at energy $-h$ in (z,w) coordinates reparametrized:

$$dLC^*K = |z|^2 dLC^*H \Rightarrow X_{LC^*K} = |z|^2 X_{LC^*H}.$$

In particular if t is the time parameter along the Kepler flow, then at this energy and for $x = (z,w)$,

$$|z|^2 \frac{dx}{dt} = |z|^2 X_{LC^*H} = X_{LC^*K},$$

so the time τ along the harmonic oscillator flow of LC^*K is reparametrized according to $\frac{dt}{d\tau} = |z|^2$.

Perturbations

The world is a complicated place and it may be overwhelming to try to understand everything. With the perturbation approach, one neglects some features of a complicated system, taking instead an approximation in its place. A good approximation should possess at least

two features. First of all, it should be simpler than the complicated system so that we can understand something about it. Second, the neglected features of the complicated system should have a sufficiently small effect so that some properties of the approximation continue to hold for the complicated system. A good approximation can then lead to some understanding of the complicated system.

For example one may have a vector field of the form $\dot{x} = X_\mu(x) = X_0(x) + \mu X_1(x) + ...$, where the vector field X_0 is understood in some way. Which properties of X_0 will persist for orbits of X_μ for μ sufficiently small? In the Hamiltonian setting, Poincaré's *general problem of dynamics* is to understand the orbits of a Hamiltonian of the form:

$$F_\mu = F_0(r) + \mu F_1(r,\theta) + \mu^2 F_2(r,\theta) + ...,$$

where $(r,\theta) \in \mathbb{R}^n \times T^n$ are conjugate coordinates. In [63], Poincaré applied implicit function theorem methods to such a problem to obtain the existence of periodic solutions to the three body problem. It took many years until Kolmogorov [45] gave conditions for quasi-periodic tori of F_0 to survive for F_μ as well.

Now we will carry out some coordinate transformations that render the three-body problem applicable to such a perturbation philosophy.

The *Jacobi coordinates* are given by figure 3.13. Taking the symplectic lift we have $P_0 = p_0 + p_1 + p_2$, $P_1 = p_1 + \sigma_1 p_2$, and $P_2 = p_2$. Note that P_0 is the linear momentum, which we will set to zero. Then the Hamiltonian for the three body problem

$$H = \sum_{i=0}^{2} \frac{|p_i|^2}{2\mu_i} - \sum_{i<j} \frac{\mu_i \mu_j}{|q_i - q_j|}$$

Figure 3.13 The Jacobi coordinates: $Q_0 = q_0$ and $Q_1 = q_1 - q_0$ and $Q_2 = q_2 - \sigma_1 q_1 - \sigma_0 q_0$ where $\sigma_i = \frac{\mu_i}{\mu_0+\mu_1}$.

becomes

$$H = \sum_{i=1}^{2} \frac{|P_i|^2}{2m_i} - \frac{\mu_0\mu_1}{|Q_1|} - \frac{\mu_0\mu_2}{|Q_2+\sigma_1 Q_1|} - \frac{\mu_1\mu_2}{|Q_2-\sigma_0 Q_1|},$$

where $\frac{1}{m_1} = \frac{1}{\mu_0} + \frac{1}{\mu_1}, \frac{1}{m_2} = \frac{1}{\mu_2} + \frac{1}{\mu_0+\mu_1}$.

We aim to view H as $H_{Kep} + H_{per}$, where H_{Kep} is the Hamiltonian for two uncoupled Kepler problems in (Q_i, P_i). This leads us to set $\mu_0\mu_1 = m_1 M_1$, from which $M_1 = \mu_0 + \mu_1$. Now we artificially introduce an $\frac{m_2 M_2}{|Q_2|}$ term and have

$$H = \sum_{i=1}^{2} (\frac{|P_i|^2}{2m_i} - \frac{m_i M_i}{|Q_i|}) + \frac{m_2 M_2}{|Q_2|} - \frac{\mu_0\mu_2}{|Q_2+\sigma_1 Q_1|} - \frac{\mu_1\mu_2}{|Q_2-\sigma_0 Q_1|},$$

which is of the form $H_{Kep} + H_{per}$ by setting $H_{per} = \frac{m_2 M_2}{|Q_2|} - \frac{\mu_0\mu_2}{|Q_2+\sigma_1 Q_1|} - \frac{\mu_1\mu_2}{|Q_2-\sigma_0 Q_1|}$.

So far we are free to choose the mass constant M_2. We will now expand H_{per} in Legendre polynomials and see that the best choice for M_2 is $\mu_0 + \mu_1 + \mu_2$.

A nice reference for the Legendre polynomials is [40]. Relevant for us here is to recall that for $z = re^{i\theta} \in \mathbb{C}$, we have

$$\frac{1}{|1-z|} = \sum_{n\geq 0} P_n(\cos\theta) r^n, \tag{3.5}$$

where $P_n(x) := \frac{1}{2^n n!} \frac{d^n}{dx^n}(x^2-1)^n$ are the *Legendre polynomials*. For example, $P_0(x) = 1, P_1(x) = x, P_2(x) = \frac{1}{2}(3x^2-1)$. They also have the property that P_n is an even function for n even and an

odd function for n odd i.e. $P_n(-x) = (-1)^n P_n(x)$.

Now we write $H_{per} = \frac{m_2 M_2}{|Q_2|}(1 - \frac{(\mu_1\mu_2)/(m_2M_2)}{|1-\sigma_0 z|} - \frac{(\mu_0\mu_2)/(m_2M_2)}{|1+\sigma_1 z|})$, where $z = Q_1/Q_2$ and expand using eq. 3.5. Then

$$H_{per} = \frac{m_2 M_2}{|Q_2|}(1 - \sum_{n\geq 0} P_n(\cos\theta) r^n (\sigma_0^n \frac{\mu_1\mu_2}{m_2M_2} + (-1)^n \sigma_1^n \frac{\mu_0\mu_2}{m_2M_2})).$$

Recall that we are going to be interested in the lunar regions: when $|Q_2| >> |Q_1|$. This expansion is nicer if we choose M_2 so that the leading term will cancel out: that is to say

$$1 - \frac{\mu_1\mu_2}{m_2M_2} - \frac{\mu_0\mu_2}{m_2M_2} = 0,$$

which implies $M_2 = \frac{\mu_2(\mu_0+\mu_1)}{m_2} = \mu_0 + \mu_1 + \mu_2$. It is also nice that the next order term vanishes with this choice of M_2:

$$\sigma_0\sigma_1 - \sigma_1\sigma_0 = 0.$$

Hence taking $M_2 = \mu_0 + \mu_1 + \mu_2$, we have

$$H_{per} = -\frac{m_2 M_2}{|Q_2|}(\sum_{n\geq 2} P_n(\cos\theta) r^n (\sigma_0^n\sigma_1 + (-1)^n \sigma_0\sigma_1^n)),$$

or by setting $\sigma_n = \sigma_0^{n-1} + (-1)^n \sigma_1^{n-1}$ and pulling out a $\sigma_0\sigma_1$ factor, this is

$$H_{per} = -\mu_2 m_1 \sum_{n\geq 2} \sigma_n P_n(\cos\theta) \frac{|Q_1|^n}{|Q_2|^{n+1}},$$

where $\theta = \angle(Q_1, Q_2)$.

Next we will consider some averaging arguments in the lunar regions, where $\frac{a_1}{a_2} = O(\varepsilon)$. First, however, let us observe that this 'averaging method' is really based off a nice canonical change of coordinates, namely those coming from the Hamiltonian flows of auxillary functions. To illustrate let us consider Poincaré's general problem of dynamics $F_\mu = F_0(r) +$

$\mu F_1(r,\theta)+...$ and let G be an auxillary Hamiltonian with Hamiltonian flow ϕ_t. Then a Taylor expansion of $F_\mu \circ \phi_\mu$ in μ leads to

$$F_\mu \circ \phi_\mu = F_\mu + \mu\{F_\mu, G\} + \frac{\mu^2}{2}\{F_\mu, \{F_\mu, G\}\} + O(\mu^3)$$

$$= F_0 + \mu(F_1 + \{F_0, G\}) + \mu^2(F_2 + \{F_1, G\} + \frac{1}{2}\{F_0, \{F_0, G\}\}) + O(\mu^3).$$

If we expand $F_1 = \sum f_k e^{ik\cdot\theta}, G = \sum g_k e^{ik\cdot\theta}$ in Fourier series, then the μ-order term is

$$\sum (f_k + (\partial_r F_0 \cdot ik) g_k) e^{ik\cdot\theta}.$$

If F_1 is analytic in a strip of width σ then $f_k = O(e^{-\sigma|k|})$ (see [5] §5). In particular $f_k = O(\mu^2)$ for $|k| \geq K$ sufficiently large. Hence provided $\partial_r F_0 \cdot ik \neq 0$ for $|k| < K$ we may define G by the *finite* Fourier series $g_k = -\frac{f_k}{\partial_r F_0 \cdot ik}$ for $|k| < K$ and $g_k = 0$ for $|k| \geq K$ to obtain

$$F_\mu \circ \phi_\mu = F_0 + \mu f_0 + \mu^2(F_2 + \{F_1, G\} - \frac{1}{2}\{F_0, F_1\}) + O(\mu^3), \tag{3.6}$$

where $f_0 = \frac{1}{(2\pi)^n}\int_{T^n} F_1 \, d\theta$ is the average of F_1.

Now let us return to the lunar regions. The Legendre polynomials have brought us to an expansion $H = H_{Kep} + H_3 + H_4 + ...$, where $H_i = O(\varepsilon^i)$. In [25] Féjoz has considered the asynchronous regime[1], showing that there is a change of coordinates through some auxiliary Hamiltonian taking us to the form

$$H = H_{Kep} + H_{Quad} + O(\varepsilon^4),$$

[1] Where the inner body rotates much faster than the outer body. The lunar regions are contained in this asynchronous regime when the angular momentum is zero.

where $H_{Quad} = \frac{1}{(2\pi)^2}\int_{T^2} H_3 \, d\lambda_1 d\lambda_2$ is the average of H_3 over the fast variables. Moreover in [25] Appendix C, he computes

$$H_{Quad} = -\frac{\mu_2 m_1}{8}\frac{a_1^2}{a_2^3}\frac{2+3e_1^2}{\varepsilon_2^3}.$$

In the lunar regions, this term is the dominant term of the secular dynamics and one can compute from the dynamics of $H_{Kep} + H_{Quad}$ that $\dot{\ell}_1 = n_1(1+O(a^3)), \dot{\ell}_2 = n_2(1+O(a^2)), \dot{g} = O(a^3)$, which we will use in some estimates above.

We will also use above the following expansion of H_{Quad} in 'polar Poincaré' variables obtained as follows. Define ε_i by $e_i^2 + \varepsilon_i^2 = 1$ with ε_i chosen to have the same sign as G_i. Then $G_i = \Lambda_i\varepsilon_i, \rho_i = \Lambda_i(1+\varepsilon_i)$ and $C = \Lambda_1\varepsilon_1 + \Lambda_2\varepsilon_2$. Taking angular momentum zero, $C = 0$, implies that $\varepsilon_2 = -\frac{\Lambda_1}{\Lambda_2}\varepsilon_1$, where $\varepsilon_1 = \frac{\rho_1}{\Lambda_1} - 1$, so that $H_{Quad} = -\frac{m_1\mu_2}{8}\frac{a_1^2}{a_2^3}\frac{5-3\varepsilon_1^2}{\varepsilon_2^3}$ where

$$5 - 3\varepsilon_1^2 = 2 + 6\frac{\rho_1}{\Lambda_1} - 3\frac{\rho_1^2}{\Lambda_1^2}$$

and

$$\frac{1}{\varepsilon_2^3} = \frac{\Lambda_2^3}{\Lambda_1^3}\frac{1}{(1-\frac{\rho_1}{\Lambda_1})}^3 = \frac{\Lambda_2^3}{\Lambda_1^3}(1 + 3\frac{\rho_1}{\Lambda_1} + 6\frac{\rho_1^2}{\Lambda_1^2} + ...).$$

Hence

$$H_{Quad} = -\frac{m_1\mu_2}{8}\frac{a_1^2}{a_2^3}\frac{\Lambda_2^3}{\Lambda_1^3}(2 + 12\frac{\rho_1}{\Lambda_1} + 15\frac{\rho_1^2}{\Lambda_1^2} + ...),$$

or as we use above:

$$H_{Quad} = \mathfrak{m}(\frac{\Lambda_1}{\Lambda_2^3} + \frac{6}{\Lambda_2^3}\rho_1 + O(\rho_1^2)), \tag{3.7}$$

where $\mathfrak{m}$ is some constant depending on the masses.

Last in this appendix, we will do some computations used above for the continuation of periodic orbits. Namely, we will compute F_{res}'s dependence on φ_1. This involves averaging

$\Lambda_0 F_{comp}$, which in the lunar regions has dominant terms (see eq. 3.6)

$$H_4 + \{H_3, G\} - \frac{1}{2}\{H_{Kep}, H_3\},$$

where we take the Legendre expansion of $H_{per} = H_3 + H_4 + ...$

Let us average these terms over the orbit (eq. 3.6 from §3) to obtain $F_{res}(J_1 = 0, \xi_1^o, \eta_1^o, \varphi_1)$. Since we only need to show this function has a non-degenerate zero as a function of φ_1, we write $\approx$ for terms that are equivalent mod terms that do not depend on φ_1. First, we have

$$\int_0^{2\pi/\omega_2^o} H_4 \, ds \approx \int_0^{2\pi/\omega_2^o} P_3(\cos((k_1+k_2)\omega_2^o s - (h_1+h_1)\varphi_1) \, ds + O(e_i),$$

since $\theta = \lambda_2 - \lambda_1 + O(e_i) = (k_1+k_2)\varphi_2 - (h_1+h_2)\varphi_1 + O(e_i)$. Now a change of variables yields

$$\int_0^{2\pi/\omega_2^o} H_4 \, ds \approx \int_{-(h_1+h_2)\varphi_1}^{2\pi(k_1+k_2)-(h_1+h_2)\varphi_1} P_3(\cos\theta) \, d\theta + O(e_i) \approx \int_0^{2\pi(k_1+k_2)} P_3(\cos\theta) \, d\theta + O(e_i) \approx O(e_i).$$

Likewise, we have

$$\int_0^{2\pi/\omega_2^o} \{H_{Kep}, H_3\} \, ds \approx O(e_i).$$

Now let ϕ_t be the flow of G so that $\{H_3, G\} = \frac{d}{dt}|_0 H_3 \circ \phi_t$. We will average first and then compute the derivative. That is, we will compute

$$\int_0^{2\pi/\omega_2^t} H_3(J_1^t, J_2(J_1^t), \xi_1^t, \eta_1^t, \omega_1^t s + \varphi_1^t, \omega_2^t s) \, ds,$$

where the t superscripts denote the flow of G with initial conditions $J_1 = 0, \xi_1^o, \eta_1^o, \varphi_1$. This integral is equivalent mod terms not depending on φ_1 to

$$\int_0^{2\pi/\omega_2^t} \cos(2((k_1+k_2)\omega_2^t - (h_1+h_2)\omega_1^t)s - 2(h_1+h_2)\varphi_1^t) \, ds + O(e_i)$$

$$\approx \sin(2(h_1+h_2)\varphi_1^t) - \sin(2(h_1+h_2)(2\pi\omega_1^t/\omega_2^t + \varphi_1^t) + O(e_i).$$

Under the flow of G we expand $\varphi_1^t = \varphi_1 + t\dot{\varphi} + ...$, $\omega_1^t = t\dot{\omega}_1 + ...$, $\omega_2^t = \omega_2^o + t\dot{\omega}_2 + ...$ Then expanding this integral in t we have

$$2\pi(h_1+h_2)\frac{\dot{\omega}_1}{\omega_2^o}\cos(2(h_1+h_2)\varphi_1)\ t + O(t^2) + O(e_i).$$

Now we differentiate at $t=0$ to obtain

$$\int_0^{2\pi/\omega_2^o} \{H_3, G\}\ ds \approx \cos(2(h_1+h_2)\varphi_1) + O(e_i).$$

Appendix B

This appendix follows [42, 32, 14], and contains some computations used for the JM-metric in §2. Most of the details are skipped and can be found in the references.

Some geometry

In this section we will define the curvature tensor for a Riemannian manifold and give formulas relating the curvature of conformal metrics and O'Neill's submersion formula. These are used to compute curvatures of the JM-metric.

First we will consider the geodesics and connections of differential geometry, which are based off the more familiar notions of lines and angle as determined by the metric (see figure 3.14).

A Riemannian manifold is a manifold M having a metric[1] g, which allows us to measure lengths and angles in the tangent space. A *geodesic* from p to q on M is an extremal of

[1] A smooth assignment of a symmetric positive definite bilinear form g_p on $TM_p \times TM_p$ for each $p \in M$, i.e. a smooth section of $T^*M \otimes T^*M$ that is symmetric and positive definite.

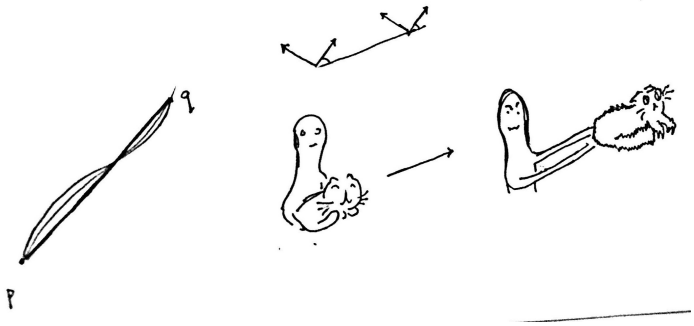

Figure 3.14 A line from p to q has minimal length among all other curves from p to q. On the right when we move objects around without changing their orientation, we use the concept of angle (it is quite difficult to do with a cat!).

the action

$$\gamma \mapsto \ell(\gamma) = \int_p^q \|\dot{\gamma}\| = \int_p^q \sqrt{g_\gamma(\dot{\gamma},\dot{\gamma})}$$

among all curves γ from p to q.

In order to compare objects in M that have been 'moved around', one needs a means to compare the tangent spaces of M at different points. A method to achieve this comparison of tangent spaces is called a *connection* on M and can be described in several ways.

Given a connection we can *parallel transport* a vector $v \in T_{c(0)}M$ over a curve $c(t)$ by requiring $v(t) \in T_{c(t)}M$ to be equivalent to v through comparison by the connection.

From a parallel transport one can define a *covariant derivative*, $\nabla : \mathfrak{X}M \times \mathfrak{X}M \to \mathfrak{X}M$ by $(X,Y) \mapsto \nabla_X Y := \frac{d}{dt}\frac{p^{-1}Y_{X^t} - Y}{t}$, where p is parallel transport along the flow X^t of X. Covariant derivatives are derivations in the second slot and $\mathcal{F}M$ linear in the first slot. Of particular interest is the Levi-Civita connection associated to g by imposing the following additional conditions. The first is that the associated connection maps $(T_pM, g_p) \to (T_qM, g_q)$ should be isometries,

and reads as

$$Xg(Y,Z) = g(\nabla_X Y, Z) + g(Y, \nabla_X Z).$$

The second is that the connection be 'torsion free' or that

$$\nabla_X Y - \nabla_Y X = [X,Y],$$

which geometrically prevents 'twisting' of vectors under parallel transport (see [32] pg. 41).

Each of the above concepts determines the connection, which is not too surprising except that a covariant derivative determines a connection. This is seen by writing out the differential equations for parallel transport (Y is parallel over $c(t)$ if $\nabla_{\dot{c}} Y = 0$) in coordinates.

The curvature tensor will measure how the parallel transport changes vectors that are transported around loops. To define it let us give this connection concept on M, g in more detail. Consider the vector bundle $\pi : TM \to M$, in a local trivialization we can take an orthonormal frame e_i with dual forms ω_i. In this local frame the parallel transport of a vector v along $c(t)$ is given by $v(t) = A(t)v$, where $A(t) \in SO(n)$ since we wish to preserve the angles of g in our identifications of tangent spaces. Now if we take a curve with $\dot{c}(0) = e_j$ and differentiate $e_i(t) = a_i^k(t)e_k$, we find

$$\nabla_{e_j} e_i = \omega_i^k(e_j)e_k,$$

where $[\omega_i^k(e_j)] = [\dot{a}_i^k] \in \mathfrak{so}(n)$ so that

$$(*) \quad \omega_i^j + \omega_j^i = 0.$$

These functions $\omega_i^j : TM \to \mathbb{R}$ are actually 1-forms from the covariant derivative's linearity in

the 1st slot. The torsion free condition on the covariant derivative implies that

$$(**)\quad d\omega_i = \omega_i^j \wedge \omega_j.$$

The two equations $(*)$ and $(**)$ are called Cartan's structural equations and determine the forms ω_i^j uniquely, which is another way to say that the Levi-Civita connection associated to g is unique.

There is yet another more general geometric interpretation of connection that will help us to better 'see' the curvature tensor. Consider a vector bundle $\tau : E \to M$. An *Ehresmann connection* on E is a horizontal subbundle H of $d\tau : TE \to TM$, which is complementary to the vertical subbundle $V = \ker d\tau$, i.e. $E = H \oplus V$. The distribution H allows us to take *horizontal lifts* (see figure 3.15) of a curve $c(t) \in M$ to a curve $\tilde{c}(t) \in E$ determined by $\tau \circ \tilde{c} = c$ and $\frac{d}{dt}\tilde{c} \in H$. Upon specifying a basepoint $(\tilde{c}(0))$, these horizontal lifts are unique. This is related to parallel transport in that having H one can define the parallel transport of $\tilde{c}(0) \in E_{c(0)}$ along c to be $\tilde{c}(t) \in E_{c(t)}$.

In our case we have the vector bundle $TM \to M$ and the covariant derivatives given in a local frame by the ω_i^j's. Let $x = (x^i)$ be coordinates on M and (x, v) coordinates on TM, with $v_i = g(v, e_i)$. Then we have coordinates on TTM as $(x, v, \mathscr{X}, \mathscr{V})$, where $\xi \in TTM$ has the form $\mathscr{X}\partial_x + \mathscr{V}\partial_v$. In these coordinates $V_{(x,v)} = (x, v, 0, \mathscr{V})$ and $H_{(x,v)} = (x, v, \mathscr{X}, \omega(\mathscr{X})v)$ where $\omega(\mathscr{X})$ is the matrix $[\omega_i^j(\mathscr{X})]$.

Now take a closed curve c in M: its lift $\tilde{c}$ being horizontal means $\tilde{c}(t) = (c(t), v(t))$ has $H \ni \frac{d}{dt}\tilde{c} = (c, v, \dot{c}, \dot{v})$ or $\dot{v} = \omega(\dot{c})v$. Hence $v(1) - v(0) = \int_{\tilde{c}} d\mathscr{V} = \int_0^1 \omega(\dot{c})v\, dt$ measures how v has changed around this loop. Note that we can view ωv as a vector valued 1-form on TTM

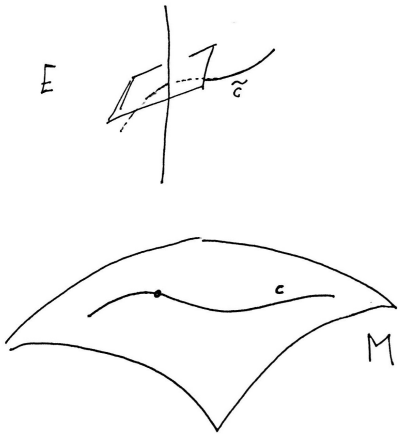

Figure 3.15 Horizontal lift in an Ehresmann connection.

with $\omega(\mathscr{X}\partial_x + \mathscr{V}\partial_v) := \omega(\mathscr{X}\partial_x)$, and then through the matrix multiplication ωv we have a vector valued 1-form.

Take c_ε to be the 'parallelogram' with vertices in M coordinates $x, x+\varepsilon u, x+\varepsilon w$ and ν a vertical curve closing up $v(1)$ to $v(0)$. Then by definition of exterior derivative we have $\int_{\tilde{c}_\varepsilon \cup \nu} \omega v = \varepsilon^2 d(\omega v)(\tilde{u},\tilde{w}) + o(\varepsilon^2)$. Now $d(\omega v)$ has ith component $dv_j \wedge \omega_i^j + v_j d\omega_i^j$, which when evaluated on $\tilde{u},\tilde{w}$ gives $(d\omega_i^j(u,v) + \omega_k^j \wedge \omega_i^k(u,v))v_j$ and captures the infinitesimal change of v upon being transported around a loop in the u,w directions. The *curvature 2-forms* are

$$(***) \quad \Omega_i^j := d\omega_i^j - \omega_i^k \wedge \omega_k^j,$$

and because of sign conventions we define the *curvature tensor* by $R_{ijkl} = -\Omega_{ij}(e_k, e_l)$. By using the definitions of ω_i^j, we have $R_{ijkl} = g(\nabla_{e_i}\nabla_{e_j}e_k - \nabla_{e_j}\nabla_{e_k}e_k - \nabla_{[e_i,e_j]}e_k, e_l)$, which is the usual way to introduce the curvature tensor and is the contraction of $R(u,v)w := \nabla_u\nabla_v w - \nabla_v\nabla_u w - \nabla_{[u,v]}w$. There is also an expression for R_{ijkl} in terms of derivatives of the components of g (see [32]).

In the case that M is two dimensional, Cartan's structural equations are nice: only ω_1^2 is non-zero. Consequently, up to symmetries, only the component R_{1212} of the curvature tensor is non-zero. This quantity is called the *Gaussian curvature*. When $n > 2$ we can define sectional curvatures of 2-planes as follows. Namely, given a point $m \in M$ and vectors $u, v \in T_pM$ the set of all geodesics tangent to $\sigma = span\{u, v\} \subset T_pM$ locally forms a surface. The Gaussian curvature of this surface is given by R_{ijij}, where ∂_i, ∂_j are an orthonormal basis for σ. We call $K(\sigma) := R_{ijij}$ the *sectional curvature* of g through the plane σ. Knowing the sectional curvatures through all 2-planes determines the full curvature tensor R_{ijkl} (see [14] pg. 13).

Figure 3.16 Another geometric interpretation of curvature: compared with rays in flat $\mathbb{R}^2$, geodesic rays spread slower with positive curvature and faster with negative curvature.

Before undertaking the computations relevant to §2, let us mention a few geometrical interpretations of these sectional curvatures so that we have some motivation to compute them. A one parameter family of geodesics, γ_s satisfies

$$\nabla_{\dot\gamma}\nabla_{\dot\gamma}V = R(\dot\gamma, J)\dot\gamma,$$

where $V = \frac{d}{ds}\gamma_s$. Such vector fields along a geodesic γ are called *Jacobi fields* (see [51]).

Since the sectional curvatures are Gaussian curvatures through certain surfaces, we will now just consider the 2-dimensional case and interpret the Gaussian curvature K. The

equation for Jacobi-fields reads

$$\ddot{y} + Ky = 0,$$

where we write the Jacobi field as $J = a(t)\dot{\gamma}(t) + y(t)\gamma(t)^{\perp}$. The Sturm-Liouville comparison theorem now allows us to see families of geodesics as in figure 3.16. Using the Jacobi fields, one can also show that the Gaussian curvature relates length and area defect of disks ([42] 5.4), that is

$$K(p) = \lim_{r\to 0} \frac{2\pi r - L(r)}{r^3}\frac{3}{\pi} = \lim_{r\to 0} \frac{\pi r^2 - A(r)}{r^4}\frac{12}{\pi},$$

where if we let $D_p(r) = \{q \in M : d_g(q,p) \leq r\}$ then $L(r)$ is the length of the boundary of $D_p(r)$ measured with g and $A(r)$ is $D_p(r)$'s area measured with g.

Now we will use Cartan's structural equations ($(*)$, $(**)$) and $(***)$ to relate the curvatures of conformal metrics. Let $\overline{g} = f^2 g$, where $f =: e^u$ is the conformal factor. Then if ω_i are dual to an orthonormal frame e_i of g, we have $\overline{\omega}_i = f\omega_i$ are dual to an orthonormal frame for $\overline{g}$. It follows that

$$d\overline{\omega}_i = du \wedge \overline{\omega}_i + e^u d\omega_i,$$

or with $du = u^j \omega_j$ we have

$$d\overline{\omega}_i = (-u^j \omega_i + \omega_i^j) \wedge \overline{\omega}_j$$

by using eqs. $(**)$ for $d\omega_i$ and that $\overline{\omega}_j \wedge \omega_i = \omega_j \wedge \overline{\omega}_i$. However, the forms $-u^j\omega_i + \omega_i^j$ are not skew (they do not satisfy $(*)$), but we can introduce the term $u^i\omega_j$, which cancels upon wedging with $\overline{\omega}_j$, and take

$$\overline{\omega}_i^j := -u^j\omega_i + u^i\omega_j + \omega_i^j$$

as the unique solution to $(*), (**)$ for $\overline{g}$.

To see the relation between the sectional curvatures, we compute in normal coordinates centered at $p \in M$, so that $(d\omega_i)_p = (\omega_i^j)_p = 0$. Then one has at p that

$$\overline{\Omega}_i^j(e_i, e_j) = \Omega_i^j(e_i, e_j) + du_j(e_j) + du_i(e_i) + \sum_{k \neq i,j} (u^k)^2,$$

or

$$f^2 \overline{K}(\overline{e}_i, \overline{e}_j) = K(e_1, e_2) - du_i(e_i) - du_j(e_j) - \sum_{k \neq i,j} (u_k)^2,$$

where we have lowered the index $(u_l = e_j(u))$ so as not to confuse any sums.

Applying this formula to the metric $U ds^2 = d\bar{s}^2$ of §2 with $u = \frac{\log U}{2}$, we have

$$U^3 \overline{K}(\sigma) = -\frac{U}{2}(\partial_1^2 U + \partial_2^2 U) + \frac{3}{4}((\partial_1 U)^2 + (\partial_2 U)^2) - \|\nabla U/2\|^2, \tag{3.8}$$

where ∂_1, ∂_2 are a ds^2 orthonormal basis for σ and $\|\cdot\|$ and ∇ are taken with respect to the ds^2 metric.

The last curvature relation in this section is O'Neill's equation for Riemannian submersions. A Riemannian submersion $\pi : (\tilde{M}, \tilde{g}) \to (M, g)$ is a submersion ($d\pi$ is onto) such that by taking $H := \ker(d\pi)^\perp$ we have $d\pi_{\tilde{m}} : H_{\tilde{m}} \to TM_m$ is an isometry for each $\tilde{m} \in \pi^{-1}(m)$. Then (see [14]) one has

$$K(\sigma) = \tilde{K}(\tilde{\sigma}) + \frac{3}{4}|[\tilde{u}, \tilde{v}]^V|^2, \tag{3.9}$$

where $\tilde{u}, \tilde{v}$ are horizontal lifts of an orthonormal basis u, v of σ and $|[\tilde{u}, \tilde{v}]^V|^2$ is the g norm of the bracket of $\tilde{u}$ and $\tilde{v}$ projected onto the vertical subspace.

To compute O'Neill's Lie bracket term of §2, we write our standard coordinates on $\mathbb{C}^3$ as $(x^1 + ix^2, ..., x^5 + ix^6)$.

Let $H_1 = X^j\partial_{x^j}$, $H_2 = Y^j\partial_{x^j} \in \mathbb{C}q^\perp$ be any horizontal vector fields and take $E = x^j\partial_{x^j}$.

Then $H_j \cdot E = H_j \cdot iE = 0$ and

$$[H_1,H_2]\cdot E = \sum_k X^j x^k \partial_{x^j} Y^k - Y^j x^k \partial_{x^j} X^k =$$

$$= \sum_k X^j(\partial_{x^j}(x^k Y^k) - \delta_j^k Y^k) - Y^j(\partial_{x^j}(x^k X^k) - \delta_j^k X^k) = \sum_k X^k Y^k - Y^k X^k = 0.$$

Likewise,

$$[H_1,H_2]\cdot iE = \sum_{k \text{ odd}} (Y^j\partial_{x^j}X^k - X^j\partial_{x^j}Y^k)x^{k+1} + (X^j\partial_{x^j}Y^{k+1} - Y^j\partial_{x^j}X^{k+1})x^k =$$

$$= 2\sum_{k \text{ odd}} -X^kY^{k+1} + X^{k+1}Y^k = 2H_1 \cdot iH_2.$$

Now if $V_a = v_a/\sqrt{U}$ are horizontal and $d\bar{s}^2$ orthonormal vectors (so v_a are horizontal and Euclidean orthonormal vectors), we have

$$|[V_1,V_2]^{\mathcal{V}_p}|^2 = ds^2_{JM}([V_1,V_2], \frac{E_p}{|p|\sqrt{U_L(p)}})^2 + ds^2_{JM}([V_1,V_2], \frac{iE_p}{|p|\sqrt{U_L(p)}})^2 =$$

$$= \frac{U_L^2}{|p|^2 U_L}(([V_1,V_2]\cdot E)^2 + ([V_1,V_2]\cdot iE)^2 = \frac{4U_L(p)(V_1\cdot iV_2)^2}{|p|^2} = \frac{4}{U_L(p)|p|^2}(v_1\cdot iv_2)^2.$$

Or

$$\frac{4}{U_L(p)|p|^2}(v_1\cdot iv_2)^2 \tag{3.10}$$

is O'Neill's bracket term, which we add to the curvature of $d\bar{s}^2$ through the horizontal plane σ with Euclidean orthonormal basis v_1, v_2.

Complex manifolds

In this section we will establish Lemma 2.6 (see [44, 19] for some more on complex manifolds). First let us set our conventions for dealing with complex manifolds.

Given a Riemannian manifold, (M^{2n}, g), with metric compatible almost complex structure J, we split the complexified tangent space into the $i, -i$ eigenspaces of $J(v \otimes \lambda) := J(v) \otimes \lambda$:

$$TM \otimes \mathbb{C} = TM' \oplus TM''.$$

In some local coordinates (x^j, y^j) on M s.t. $J(\partial_{x^j}) = \partial_{y^j}$ we then have the bases for TM' and TM'' respectively as $\partial_j := \frac{1}{2}(\partial_{x^j} \otimes 1 - \partial_{y^j} \otimes i)$ and $\overline{\partial}_j := \frac{1}{2}(\partial_{x^j} \otimes 1 + \partial_{y^j} \otimes i)$.

Now we extend the metric $\mathbb{C}$-linearly to a $\mathbb{C}$-valued symmetric bilinear form on $TM \otimes \mathbb{C}$, by $g(v \otimes \lambda, \cdot) := \lambda g(v, \cdot)$. Using the metric compatibility of J, we find $g_{ij} = g(\partial_i, \partial_j) = 0 = g_{\bar{i}\bar{j}}$ and

$$g_{i\bar{j}} = \frac{1}{2}(g(\partial_{x^i}, \partial_{x^j}) + ig(\partial_{x^i}, \partial_{y^j})) = g_{\bar{i}j},$$

and so

$$g = g_{i\bar{j}}(dz^i \otimes d\bar{z}^j + d\bar{z}^j \otimes dz^i) = 2g_{i\bar{j}} dz^i d\bar{z}^j,$$

where $dz^i = dx^i + i dy^i, d\bar{z}^i = dx^i - i dy^i$ are dual to $\partial_i, \overline{\partial}_i$.

Let $D \subset \mathbb{C}$ be a disk containing 0 and $f : D \to M$ a holomorphic map. Let K_{f^*g} be the Gaussian curvature of f^*g on D. Define

$$H_q(X) := \sup\{K_{f^*g}(0) : f : D \to M \text{ holomorphic and } f(0) = q, \mathbb{C}f'(0) = \mathbb{C}X\} \tag{3.11}$$

to be *Kobayashi's holomorphic sectional curvature*. Kobayashi's definition is motivated by interpreting the Schwartz Lemma as an inequality on curvatures of regions related by holomorphic maps. In ([44], ch. 2) Kobayashi shows that

$$H_q(X) = R_{i\bar{j}k\bar{l}} X^i \overline{X}^j X^k \overline{X}^l, \tag{3.12}$$

for a unit vector $X = X^j \partial_j$ (i.e. $g(X, \overline{X}) = 1$ by extending g $\mathbb{C}$-linearly) and where

$$R_{i\bar{j}k\bar{l}} := -\partial_k \overline{\partial}_l g_{i\bar{j}} + g^{p\bar{q}} \partial_k g_{i\bar{q}} \overline{\partial}_l g_{p\bar{j}}. \tag{3.13}$$

Now we are ready to prove Lemma 2.6.

Proof. Take an orthonormal Euclidean basis with $e_1 = (1,0,...,0) = \lambda v_1$ and $e_2 = (0,1,0,...,0) = i\lambda v_1, ...$ so that we may write the JM-metric as $(h+U)\sum \mu_j dz_j d\bar{z}_j$, where $\mu_j > 0$ are some positive constants depending on the masses.

In the real coordinates (x_j, y_j) where $z_j = x_j + iy_j$ we then have

$$K(v, iv) = \frac{R_{x_1 y_1 x_1 y_1}}{\mu_1^2 (h+U)^2},$$

where R_{ijkl} is the Riemannian curvature tensor associated to the real metric $(h+U)\sum \mu_j (dx_j^2 + dy_j^2)$. Then eq. 3.8 gives

$$R_{x_1 y_1 x_1 y_1} = \frac{\mu_1}{2}(-\Delta_1 U + \frac{(\partial_{x_1} U)^2 + (\partial_{y_1} U)^2}{h+U} - \frac{\sum_{j=2}^N \frac{\mu_1}{\mu_j}((\partial_{x_j} U)^2 + (\partial_{y_j} U)^2)}{2(h+U)}),$$

and takes the form in complex coordinates ($\partial_j = \frac{\partial}{\partial z_j} = \frac{1}{2}(\partial_{x_j} - i\partial_{y_j})$)

$$R_{x_1 y_1 x_1 y_1} = \frac{\mu_1}{2}(-4\partial_1 \overline{\partial}_1 U + \frac{4\partial_1 U \overline{\partial}_1 U}{h+U} - \frac{2\sum_{j=2}^N \frac{\mu_1}{\mu_j} \partial_j U \overline{\partial}_j U}{h+U}).$$

Now using eqs. (3.12) and (3.13) with $v = \partial_1$ and corresponding unit vector $X = \sqrt{\frac{2}{\mu_1 (h+U)}}\partial_1 = \frac{\partial_1}{\sqrt{g_{1\bar{1}}}}$, we compute

$$R_{1\bar{1}1\bar{1}} = \frac{\mu_1}{2}(-\partial_1 \overline{\partial}_1 U + \frac{\partial_1 U \overline{\partial}_1 U}{h+U}),$$

and then

$$H_q(v) = \frac{4R_{1\bar{1}1\bar{1}}}{\mu_1^2 (h+U)^2} = K_q(v, Jv) + \frac{\sum_{j=2}^N \frac{1}{\mu_j} \partial_j U \overline{\partial}_j U}{(h+U)^3}.$$

The formula in the Lemma then follows by rescaling ∂_j by $\frac{1}{\sqrt{\mu_j}}$.

□

Geodesic flows on manifolds of non-positive curvature

In this section we will explain some motivation for finding negatively curved circumstances: mainly where the symbolic dynamics comes from. We follow the lectures of A. Manning and C. Series from [8], which contain more of the details.

Consider the hyperbolic plane, $\mathbb{H}$, a complete surface of curvature -1, which can be modeled by the upper half plane $\{(x,y) : y > 0\}$ with metric $\frac{dx^2+dy^2}{y^2}$ or the unit disk $\{z \in \mathbb{C} : |z| < 1\}$ with metric $2\frac{dzd\bar{z}}{1-|z|^2}$. These two are related through the Möbius transformation $z \mapsto \frac{z-i}{z+i}$.

The *geodesic flow* of a Riemannian manifold (M,g) is the flow on its unit tangent bundle, UM, given by $g^t v = \dot{\gamma}_v(t)$, where γ_v is the geodesic with initial condition $\gamma_v(0) = \pi(v), \dot{\gamma}_v(0) = v$.

Let us first see how the geodesic flow of $\mathbb{H}$ is an Anosov flow (see figure 3.17).

The isometry group of $\mathbb{H}$ is $PSL_2(\mathbb{R}) = SL_2(\mathbb{R})/\pm I$, which acts on the upper half plane model by $\begin{bmatrix} a & b \\ c & d \end{bmatrix} z = \frac{az+b}{cz+d}$. This action extends to a free and transitive action on the unit tangent bundle. One can thus identify $U\mathbb{H}$ with the orbit of a point under this group action.

Identify $U\mathbb{H}$ with the orbit of $(i,i) \in U\mathbb{H}$. The geodesic through this point is given by

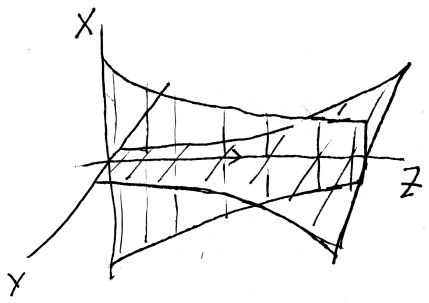

Figure 3.17 An Anosov flow, φ^t on M is one for which TM admits a splitting as $X \oplus Y \oplus Z$ with the following properties. The splitting should be invariant under φ^t: $X_{\varphi^t} = d\varphi^t X$, etc. It should be contracting along X: $\|d\varphi^t|_X\| = Ce^{-\lambda t}$ and expanding along Y: $\|d\varphi^t|_Y\| = Ce^{\lambda t}$ for some $C, \lambda > 0$. And the direction Z is the direction of the flow: $Z = \frac{d}{dt}\varphi^t$. Such flows have sensitive dependence on initial conditions. The X and Y spaces are called the stable and unstable directions.

$\gamma(t) = ie^t = \begin{bmatrix} e^{t/2} & 0 \\ 0 & e^{-t/2} \end{bmatrix} i$, or under our identification,

$$g^t(I) = \begin{bmatrix} e^{t/2} & 0 \\ 0 & e^{-t/2} \end{bmatrix}.$$

To see the Anosov splitting of $U\mathbb{H}$ under g^t, we use the horocycle flow (see figure 3.18).

The geodesics forward asymptotic to γ have initial condition $(t+i, i) = \begin{bmatrix} 1 & t \\ 0 & 1 \end{bmatrix} = h^t_+(I)$. While those backwards asymptotic to γ are identified through $h^t_-(v) = -h^{-t}_+(-v)$ and since $v \mapsto -v$ at i is achieved through $\begin{bmatrix} 0 & -1 \\ 1 & 0 \end{bmatrix}$, we have $h^t_-(I) = \begin{bmatrix} 1 & 0 \\ t & 1 \end{bmatrix}$.

Now we define our Anosov splitting at (i,i) to be made up of the curves tangent to

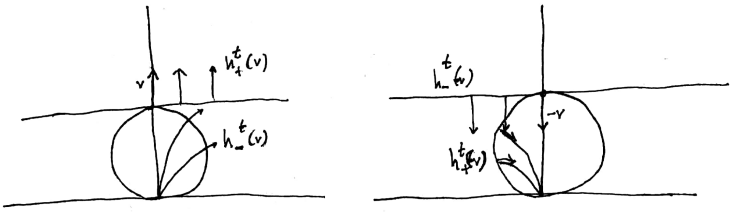

Figure 3.18 Geodesics tangent to the normal vectors of the 'circle with a point at infinity' $\lim_{r\to\infty}\{z \in \mathbb{H} : d(z,\gamma_v(r)) = r\}$ are forward asymptotic to γ_v. Likewise the geodesics tangent to the normals of $\lim_{r\to\infty}\{z \in \mathbb{H} : d(z,\gamma_v(r)) = r\}$ are backwards asymptotic to γ_v. The horocycle flows, h_+^t, h_-^t, slide the vector v along these inner normals. We have $-h_-^t(-v) = h_+^{-t}(v)$.

$g^t(I), h_+^t(I), h_-^t(I)$. Since we are in a Lie group, we push these around by left multiplication to define a splitting over $U\mathbb{H}$. We give $U\mathbb{H}$ the Euclidean metric at (i,i) by $\| \begin{bmatrix} a & b \\ c & -a \end{bmatrix} \| = a^2 + b^2 + c^2$ and push this around by left multiplication to define a metric on $U\mathbb{H}$.

Then it suffices to show this splitting is contracting and expanding along the horocycle flows. We compute that $\|dg^t(\frac{d}{ds}h_+^s(v))\| = \|g^{-t}\begin{bmatrix} 0 & e^{-t/2} \\ 0 & 0 \end{bmatrix}\| = e^{-t}$, and likewise $\|dg^t(\frac{d}{ds}h_-^s(v)\| = e^t$. Hence the geodesic flow of $\mathbb{H}$ is indeed an Anosov flow.

Consequently any surface of constant negative curvature is, by the Cartan-Hadamard theorem, a quotient of $\mathbb{H}$ and so also has an Anosov geodesic flow. It has been shown that even when the sectional curvatures of an n-dimensional Manfold are negative (and not necessarily constant) [3] that the geodesic flow is also Anosov.

In particular, a theorem of Bowen [12] states that any Anosov flow admits a Markov partition, allowing one to describe the dynamics by symbolic dynamics. For quotients of $\mathbb{H}$, this symbolic dynamics comes from a 'tiling sequence', which describes the free homotopy class

realized by the geodesic (see figure 3.19)

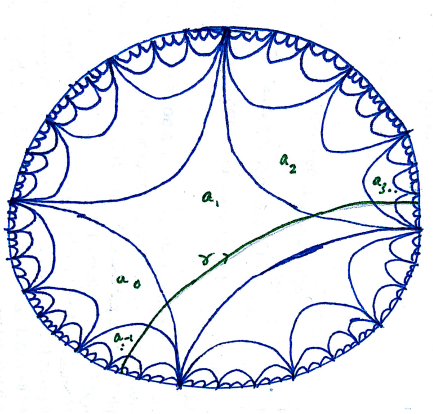

Figure 3.19 Upon quotienting by a discrete subgroup the Hyperbolic plane is tiled into fundamental regions (analogous to considering the torus $\mathbb{R}^2/\mathbb{Z}^2$ as a tiling of $\mathbb{R}^2$). Here we have a punctured torus as a quotient of $\mathbb{H}$, each geodesic is uniquely determined by the 'sides' or 'tiles' it cuts through (we labeled the tiles here as $...a_{-1}, a_0, a_1, ...$). See the famous pictures of Escher for more tilings:)

One gets the feeling that our hopes for negatively curved circumstances need not be dashed by the mixed curvature found for the $N > 3$ body problems above. Rather the question should be whether or not these geodesic flows are Anosov. We mention the results of Klingenberg [43], who has shown that many of the properties of negatively curved manifolds persist for those with an Anosov geodesic flow. In particular, if the geodesic flow is Anosov there can be at most one geodesic in each free homotopy class (the uniqueness property we sought above).

The following examples give some extremes of the relation between mixed curvatures and Anosov geodesic flows.

EXAMPLE (Due to Daniel Visscher, see figure 3.20) To obtain an example of an

Anosov geodesic flow on a compact surface having mixed curvature (embedded in $\mathbb{R}^3$!), consider first two planes and connect them with many negatively curved tubes. The resulting geodesic flow is Anosov. One may then slowly curve these sheets around to form two gigantic tori in $\mathbb{R}^3$ connected by tubes. The resulting surface still has an Anosov geodesic flow (by structural stability of Anosov flows). Being embedded in $\mathbb{R}^3$ compactly, such a surface must have mixed curvature.

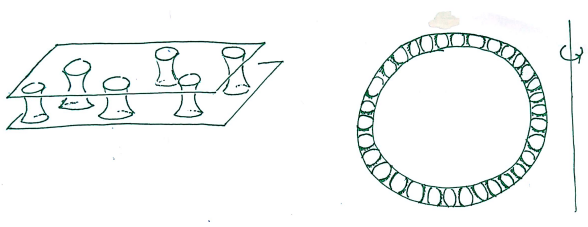

Figure 3.20 A compact surface in $\mathbb{R}^3$ with mixed curvature and an Anosov geodesic flow.

EXAMPLE Give $\mathbb{R}^3\backslash\{x=y=0\}$ the following metric: $\frac{dx^2+dy^2+dz^2}{x^2+y^2}$. Along the $\partial_\theta, \partial_z$ directions one can compute that the curvature is positive. In the other directions, we have a 'book' of hyperbolic planes on each vertical slice $\theta = \tan y/x = cst.$. While on each horizontal slice, $z = cst.$ is metrically a 'cylinder'. These slices are totally geodesic, so we have negative and zero curvature along them. In this mixed curvature metric many geodesics realize the same homotopy class (waists of the cylinders), so the flow is not Anosov (see figure 3.21).

Last we will mention Preissman's theorem (see [31] for a nice geometric proof). This theorem states that when (M,g) is a complete negatively curved manifold, then if γ_1 and γ_2 are two geodesics and $[\gamma_i]$, their representatives in the fundamental group one must have

$$[\gamma_1]\cdot[\gamma_2] \neq [\gamma_2]\cdot[\gamma_1].$$

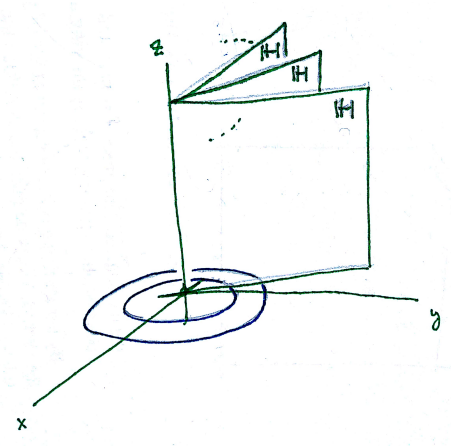

Figure 3.21 This book of $\mathbb{H}$'s in $\mathbb{R}^3 \setminus \{z\text{-axis}\}$ has mixed curvature and is not an Anosov flow since in the xy-plane circles centered at the origin are geodesics.

In other words there is no $\mathbb{Z}^2$ in the fundamental group realized by geodesics.

This is relevant to the above work since it makes the mixed curvature of Theorem 1 plausible, only when $N > 3$ are there commuting homotopy classes available (see figure 3.22) giving a chance to preclude non-positive curvature by realizing such classes.

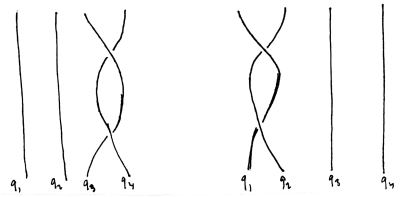

Figure 3.22 Commuting free homotopy classes in the 4-body problem. Are they realized by solutions?

Due to the positive curvature in the orthogonal directions to the collinear 4-body problem, one can imagine that realizing such commuting classes is possible by a geodesic with a small velocity component in this orthogonal direction, which shadows a collinear geodesic. As two bodies come close to a collision they make a quick revolution around each other to

switch their ordering and jump into another triangle (figure 2.2). If one can continue shadowing the collinear orbits in such a way as to make a closed loop, the classes of figure 3.22 may be realizable.

Bibliography

[1] A. Albouy, *On the force fields which are homogeneous of degree -3* Paru dans Extended Abstracts Spring 2014, Volume 4 of the series Trends in Mathematics pp. 3-7

[2] A. Albouy, *Some classical integrable problems*, Lecture in Hanoi.

[3] D.V. Anosov. *Geodesic flows on closed Riemannian manifolds of negative curvature*. Trudy Matematicheskogo Instituta Imeni VA Steklova 90 (1967): 3-210.

[4] V.I. Arnold, *Mathematical Methods of Classical Mechanics*, Springer; 2nd edition (1997).

[5] V.I. Arnold, *Lectures on partial differential equations*, Springer Science & Business Media, 2013.

[6] V.I. Arnold, V.V. Kozlov, A.I. Neishtadt, *Mathematical aspects of classical and celestial mechanics*, Springer (2002).

[7] M. Barbosu, B. Elmabsout, *Courbures de Riemann dans le probléme plan des trois corps - Stabilité*, Comptes Rendus de l'Acadèmie des Sciences - Series IIB - Mechanics - Physics - Astronomy, Vol. 327 issue 10, pp 959-962 (1999).

[8] A. Beardon, M. Keane, C. Series, *Ergodic Theory Symbolic Dynamics and hyperbolic spaces*, Oxford Science publications (1991).

[9] A. Besse, *Manifolds all of whose geodesics are closed*, Springer (1978).

[10] G.D. Birkhoff, *Dynamical Systems*, American Mathematical Society (1927).

[11] S. Bolotin, P. Negrini, *Variational approach to second species periodic solutions of Poincaré of the 3 body problem*, arXiv:11-4.2288 (2011).

[12] R. Bowen. *Symbolic dynamics for hyperbolic flows*. American journal of mathematics 95.2 (1973): 429-460.

[13] A. Bruno, *The Restricted three-body problem: Plane Periodic Orbits*, de Gruyter (1994).

[14] J. Cheeger, D. Ebin. *Comparison theorems in Riemannian geometry*. Vol. 365. American Mathematical Soc., 2008.

[15] K.C. Chen, *Action-Minimizing Orbits in the Parallelogram Four-Body Problem with Equal Masses*, Archive for Rational Mechanics and Analysis July 2001, Volume 158, Issue 4, pp 293?31.

[16] A. Chenciner, *Poincaré and the three-body problem*, Sminaire Poincar (Bourbaphy) XVI, p. 45-133 (2012)

[17] A. Chenciner, *Le probléme des N corps et le systéme solaire*, Sciences et Avenir hors-srie 'La dixime plante' numro 145.

[18] A. Chenciner, R. Montgomery, *A remarkable periodic solution of the three body problem in the case of equal masses*, Annals of Mathematics, 152, pp. 881-901 (2000)

[19] Chern, Shiing-Shen, et al. *Complex manifolds without potential theory*. Vol. 15. Princeton: van Nostrand, 1967.

[20] M. Chupin. *Interplanetary transfers with low consumption using the properties of the restricted three body problem*. Optimization and Control [math.OC]. Paris 6, 2016.

[21] H. Dumas, *The KAM story*, World Scientific Publishing Company, (2014).

[22] J. Féjoz, *Sur le théorème de Bertrand (d'après Michael Herman)*, Michael Herman Memorial Issue, Ergodic Theory Dyn. Sys.24:5 (2004) 1583?1589

[23] J. Féjoz, *Le probléme de la stabilite du Systeéme solaire, de Lagrange á nos jours*, Deux cents ans aprs Lagrange (IHP, 28 juin 2013).

[24] J. Féjoz, *The N-body problem*, Modified version of a chapter in Celestial Mechanics (ed. Alessandra Celletti), 2015

[25] J. Féjoz, *Quasi-periodic motions in the planar N-body problem*, J. Differential Equations 183 (2002), no. 2, 303?341

[26] J. Féjoz, *Global Secular Dynamics in the planar three-body problem*, Celestial Mech. Dynam. Astronom. 84 (2002), no. 2, 159?195

[27] J. Féjoz, *On the action angle coordinates and Poincare coordinates*, Regular and Chaotic

Dynamics, Special Issue dedicated to Alain Chenciner on the occasion of his 70th anniversary, 18:6 (2013), 703?718

[28] J. Féjoz, *An introduction to KAM theory, with a view to celestial mechanics*, Variational methods in imaging and geometric control Radon Series on Comput. and Applied Math. 18, de Gruyter, 2016

[29] W. Gordon, *Conservative Dynamical Systems involving Strong Forces*, Transactions of the American Mathematical Society, vol. 204 pp 113-135, (1975).

[30] W. Gordon, *A minimizing property of Keplerian orbits*, American Journal of Mathematics Vol. 99, No. 5 (Oct., 1977), pp. 961-971

[31] A. Grant, *Preissman's theorem*, an REU paper.

[32] D. Gromoll, W. Klingenberg, W. Meyer, *Riemannsche Geometrie im Großen*, Springer-Verlag (1968).

[33] J. Hadamard, *Les surfaces à courbures opposées et leurs lignes géodésiques*, Journal de mathématiques pures et appliquées 5e série, tome 4 p. 27-74 (1898).

[34] J. Hadamard, *Sur un Mémoire de M. Sundman*, Bulletin des Sciences Mathématiques, 39, pp. 249-264 (1915).

[35] E. Hopf, *Statistik der geodätischen Linien in Mannigfaltigkeiten negativer Krümmung*, Hirzel (1939).

[36] C. Jackman, *No Hanging out in neighborhoods of infinity*, Celestial Mech. Dynam. Astronomy. Vol. 128 (2017), pp 183-195.

[37] C. Jackman, J. Melendez, *On the sectional curvature along relative equilibria*, arXiv:1703:08445, (2017).

[38] C. Jackman, J. Melendez, *Hyperbolic Shirts fit a 4-body problem*, Journal of Geometry and Physics, Vol. 123 (2018) pg. 173-183.

[39] C. Jackman, R. Montgomery, *No Hyperbolic Pants for the 4-body problem with Strong Potential*, Pacific Journal of Mathematics, Vol. 280 (2016), No. 2, 401-410.

[40] K. Jänich. *Analysis fur Physiker und Ingenieure: Funktionentheorie, Differentialgleichungen, Speziell Funktionen*. Springer, 1983.

[41] S. Kaplan, M. Levi, R. Montgomery, *Making the moon reverse its orbit: stuttering in the planar three body problem*, Discrete and Continuous Dynamical Systems series B, (Simfest issue), vol. 10, no. 2/3, 2008

[42] W. Klingenberg, *Eine Vorlesung über Differentialgeometrie*, Springer-Verlag (1973).

[43] W. Klingenberg. *Riemannian manifolds with geodesic flow of Anosov type*. Annals of Mathematics (1974): 1-13.

[44] S. Kobayashi. *Hyperbolic complex spaces*. Vol. 318. Springer Science & Business Media, 2013.

[45] A.N. Kolmogorov, *On conservation of conditionally periodic motions for a small change in Hamilton's function*, Dokl. Akad. Nauk SSSR 98 (1954) pp.527-530

[46] Liu Cixin, *Remembrance of Earth's Past trilogy*, Tor Books (2017).

[47] J-P. Marco, L. Niedermann, *Sur la construction des solutions de second espéce dans le probléme des trois corps*, Annales de l'I.H.P Physique théoretique, Vol. 62 (1995) pp 211-249

[48] C. Marchal, *The three-body problem*, Elsevier Science (1990).

[49] R. McGehee. *Triple collision in Newtonian gravitational systems*. Dynamical Systems, Theory and Applications. Springer, Berlin, Heidelberg, 1975. 550-572.

[50] K. Meyer, *Periodic solutions of the N-body problem*, Springer Lecture Notes in Mathematics, 1999.

[51] J. Milnor. *Morse Theory*. (AM-51). Vol. 51. Princeton university press, 2016.

[52] R. Moeckel, *Some qualitative features of the three-body problem*, pp. 1-21 in Hamiltonian Dynamical Systems, Proceedings of a summer research conference held June 21-27, 1981. Edited by Kenneth R. Meyer and Donald G. Saari. Contemporary Mathematics 81. American Mathematical Society, 1988.

[53] R. Moeckel, R. Montgomery, *Realizing All Reduced Syzygy Sequences in the Planar Three-Body Problem*, Nonlinearity 28, 2015.

[54] R. Montgomery, *Hyperbolic pants fit a 3-body problem*, Ergodic theory and Dynamical Systems, Volume 25, 921-947, 2005.

[55] R. Montgomery, *The three body problem and the shape sphere*, Amer. Math. Monthly, v 122, no. 4, pp 299-321 , April 2015.

[56] R. Montgomery, *The N-body problem, the braid group and action minimizing orbits*, Nonlinearity, vol. 11, no. 2, 363-376, 1998.

[57] J. Moser. *Regularization of Kepler's problem and the averaging method on a manifold*. Communications on Pure and Applied Mathematics 23.4 (1970): 609-636.

[58] Ong Chong Pin, *Curvature and Mechanics*, Advances in Mathematics, Vol. 15, issue 3, 1975 pp. 269-311.

[59] G. Paternain, *Geodesic Flow*, Birkhauser 1964.

[60] H. Poincaré, *Sur les orbites périodiques et le principe d'action moindre*, C.R.A.S., t. 123, pp 915-918, 1896.

[61] H. Poincaré, *Surs les courbes definies pour une equation differentiale I*, Journal de mathématiques pures et appliquées 3e série, tome 7 (1881) pp 375-422

[62] H. Poincaré, *Sur la stabilite du systeme solaire*, Annuaire du Bureau des longitudes, 1898, B1?B16; Revue scientifique 9(20), 1898, 609?613.

[63] H. Poincaré, *Les Nouvelles Methodes des Mechaniques Celestes I, II, III*, Gauthiers-Villars 1892,

[64] H. Pollard, *Celestial Mechanics*, Prentice Hall (1966).

[65] G. Reeb, *Propriétés des trajectoires de certains systèmes dynamiques*, Séminaire Bourbaki (Décembre 1949).

[66] K. Sundman, *Mémoire sur le problème des trois corps*. Acta mathematica 36.1 (1913): 105-179.

[67] J. Van Velsen, *On the Riemann curvature of conservative systems in classical mechanics*, September 1978, Physics Letters A 67(5-6):325-327

[68] J. Van Velsen, *The Average Riemann curvature of conservative systems in classical mechanics*, January 1999, Journal of Physics A General Physics 14(7):1621